



# Correlation between trace element concentrations in the blood of female hawksbill (*Eretmochelys imbricata*) and egg quality in nesting populations of São Tomé Island

Inês F.C. Morão<sup>a,b,\*</sup>, Tiago Simões<sup>a</sup>, Roger B. Casado<sup>a</sup>, Sara Vieira<sup>c,d</sup>,  
Betânia Ferreira-Airaud<sup>c,d</sup>, Ilaria Caliani<sup>e</sup>, Agata Di Noi<sup>e,f</sup>, Silvia Casini<sup>e,g</sup>,  
Maria C. Fossi<sup>e,g</sup>, Marco F.L. Lemos<sup>a</sup>, Sara C. Novais<sup>a,\*\*</sup>

<sup>a</sup> MARE - Marine and Environmental Sciences Centre & ARNET - Aquatic Research Network, ESTM, Politécnico de Leiria, Portugal

<sup>b</sup> Faculdade de Ciências & CESAM, Universidade de Lisboa, Campo Grande, 1749-016, Lisboa, Portugal

<sup>c</sup> Associação Programa Tatò, Avenida Marginal 12 de Julho, Ilha de São Tomé, Cidade de São Tomé, Democratic Republic of Sao Tome and Principe

<sup>d</sup> Centro de Ciências do Mar (CCMAR), Universidade do Algarve, Campus de Gambelas, 8005-139, Faro, Portugal

<sup>e</sup> Department of Physical, Earth and Environmental Sciences, University of Siena, via Mattioli, 4, 53100, Siena, Italy

<sup>f</sup> Santa Chiara Lab, University of Siena, via Valdimontone, 1, 53100, Siena, Italy

<sup>g</sup> NBFC, National Biodiversity Future Center, Palermo, Italy

## ARTICLE INFO

### Keywords:

Egg reserves  
Erythrocyte nuclear abnormalities  
Fatty acids  
Metals  
Reptiles  
Wildlife ecotoxicology

## ABSTRACT

Metals and metalloids can pose a significant threat to sea turtles, as these contaminants tend to accumulate in their bodies over time, due to their long lifespans and varied feeding habits. São Tomé and Príncipe's archipelago hosts the last remaining rookery for hawksbill sea turtles (*Eretmochelys imbricata*) in the region. The study aimed to determine the levels of metals and metalloids accumulated by this population and to investigate their possible genotoxicity in nesting females' blood as well as potential effects on their eggs in terms of morphometric characteristics and the quality of their lipidic reserves, essential for embryo development. Higher levels of Hg were found to be correlated with increased "lobed-shaped nuclei" in erythrocytic count, suggesting genotoxicity effects in this population. Higher levels of Se were correlated with thicker and heavier eggshells, while Pb levels were associated with the reduction of the egg's diameter. Metal contamination in females' blood significantly affected yolk polar fatty acids. Significant negative correlations were found between general metal contamination (PLI) and saturated fatty acids (SFA), while positive correlations were observed for essential omega-6 fatty acids (n6), mostly influenced by Cu, Fe, and Hg concentrations. This suggests that these omega-6 fatty acids are being synthesized from SFA, potentially indicating stress response by metal exposure. The present results point to some potential alterations in the normal embryonic development of these turtle eggs, influenced by metal contamination, which should raise some concerns about the future of this critically endangered species and call for additional conservation efforts in the region.

## 1. Introduction

The hawksbill sea turtle (*Eretmochelys imbricata*), listed as critically endangered in the IUCN Red List, is primarily found in tropical and subtropical waters, playing a crucial role in maintaining healthy coral reefs by feeding mainly on sponges (Baumbach et al., 2022; Horne et al., 2023). However, this species faces significant threats, including bycatch, coastal development, climate change, excessive targeting in the illegal

shell trade and pollution, which have contributed to a substantial global populations decline over the last century (Arantes et al., 2020; Fuentes et al., 2023; Hawkes et al., 2009; Horne et al., 2023; Mortimer and Donnelly, 2008).

One of the most vulnerable populations is found in São Tomé and Príncipe archipelago, which hosts the last remaining rookery of hawksbill sea turtles in the Gulf of Guinea region (Ferreira et al., 2018; Ferreira-Airaud et al., 2022). An estimated 170 to 300 female hawksbill

\* Corresponding author. Edifício CETEMARES, Avenida do Porto de Pesca, 2520 – 630, Peniche, Portugal.

\*\* Corresponding author.

E-mail addresses: [ines.morao@ipleiria.pt](mailto:ines.morao@ipleiria.pt) (I.F.C. Morão), [sara.novais@ipleiria.pt](mailto:sara.novais@ipleiria.pt) (S.C. Novais).

<https://doi.org/10.1016/j.envres.2025.121594>

Received 19 December 2024; Received in revised form 24 March 2025; Accepted 9 April 2025

Available online 17 April 2025

0013-9351/© 2025 The Authors. Published by Elsevier Inc. This is an open access article under the CC BY-NC-ND license (<http://creativecommons.org/licenses/by-nc-nd/4.0/>).

sea turtles nest in the archipelago, with the Rolas islet being the primary nesting site for this species (Ferreira-Airaud et al., 2024). This population is characterised by a unique genetic haplotype and exhibits low genetic variability (Monzón-Argüello et al., 2011), placing it among the eleven most threatened hawksbill populations worldwide (Wallace et al., 2011). Given its critical conservation status, understanding the environmental pressures affecting this population is essential for its long-term survival.

The southern region of São Tomé Island, where Rolas Islet is located, is characterised by agricultural activities, including the cultivation of oil palm, cassava, cocoa, and other crops (Palmeirim et al., 2024), which can contribute to soil contamination by metals. Mangrove ecosystems in this southern area show evidence of pollution by arsenic (As), chromium (Cr), zinc (Zn), lead (Pb), and copper (Cu), primarily due to agricultural runoff and other human activities (Afonso et al., 2023). Additionally, local fishing practices contribute to pollution through the use of anti-fouling paints, while domestic activities, such as washing clothes with detergents in rivers, introduce further harmful substances (Afonso et al., 2022, 2023). Given its proximity to these pollution sources, Rolas Islet may be exposed to these contaminants, posing potential risks to the nesting hawksbill turtle population.

These marine reptiles are vulnerable to the accumulation of persistent pollutants, such as organochlorine pesticides, metals and metalloids, in their tissues due to their long lifespans, migratory behaviors and feeding habits (Finlayson et al., 2016; Fuentes et al., 2023; Ross et al., 2017). Although metals and metalloids can be toxic, they differ in their environmental persistence and biological effects (Tchounwou et al., 2012). Metals, such as mercury (Hg) and cadmium (Cd), accumulate in tissues over time, leading to chronic toxicity (Jannetto and Cowl, 2023; Tchounwou et al., 2012), whereas metalloids like arsenic (As) and selenium (Se) interact differently with biological systems (Kesawat et al., 2020). Selenium is essential in trace amounts but becomes toxic at higher concentrations (Zwolak and Zaporowska, 2012), while arsenic has no known biological role and is toxic even at low levels (Tchounwou et al., 2012).

These contaminants have been shown to have detrimental effects on various physiological processes in sea turtles, significantly impacting their health and reproductive success. For example, Hg exposure has been associated with compromised immune function (Day et al., 2007), while Hg, Pb and Cd have demonstrated genotoxicity effects, leading to alterations in their gene expression patterns, particularly in oxidative stress-related genes such as catalase and metal transport proteins like metallothioneins (Casini et al., 2018; Cortés-Gómez et al., 2018; Morão et al., 2022, 2024). Furthermore, certain metal pollutants, such as hexavalent chromium [Cr(VI)] are known to induce cytotoxicity (Speer et al., 2018), which can further affect cellular integrity and function.

Sea turtles invest significant energy and resources toward reproduction (Gatto et al., 2020), carefully selecting appropriate nesting sites, excavating nests, and laying multiple clutches per nesting season (Gatto et al., 2020; Miller, 1997). Eggs represent a considerable reproductive investment as they provide all the necessary nutrients for the development of future generations of sea turtles (Le Gouvello et al., 2020; Miller, 1997). The process of embryonic development within reptile eggs involves intricate mechanisms that begin with the supply of essential nutrients from the egg (Ackerman, 1997). These yolk-derived nutrients include inorganic ions (e.g., calcium), vitamins (e.g., A and E), water, hormones (e.g., steroids) and proteins such as lipovitellin and phosvitin, which are essential for embryonic growth and metabolism (Thompson and Speake, 2002; Van Dyke and Griffith, 2018). Additionally, lipids including phospholipids and triglycerides, along with their functional components (e.g., fatty acids), serve as crucial energy sources and essential building blocks for cellular activities (Lawniczak and Teece, 2009). These components support the development of tissues, organs, and physiological systems throughout embryogenesis (Van Dyke and Griffith, 2018), underscoring their vital role in maintaining egg quality and ensuring proper embryonic development.

However, the balance of these yolk-derive components can be affected by environmental factors, such as metal contamination (Tanabe et al., 2022; van de Merwe et al., 2009). Female sea turtles accumulate metals both through recent exposure (reflected in their blood which also suggests a risk of transfer via lipid mobilization) and long-term accumulation in fat stores and organs such as the liver (Yipel et al., 2017; Villa et al., 2017). During vitellogenesis, when energy reserves are mobilized to form egg yolks, stored contaminants are also transferred, potentially affecting embryonic development and reproductive success (Guirlet et al., 2008; Páez-Osuna et al., 2011).

A few studies have addressed metal and metalloid contamination in nesting sea turtles and maternal transfer to their eggs, highlighting their potential impact on reproductive success (Ehsanpour et al., 2014; Guirlet et al., 2008; Miguel et al., 2023; Perrault et al., 2013; Páez-Osuna et al., 2010b; Sakai et al., 1995; Simões et al., 2019). For instance, both Hg and Se have been linked to reduced reproductive success in leatherback turtles (Perrault et al., 2013). Additionally, nickel (Ni) levels in blood have been associated with smaller clutch sizes (Simões et al., 2019). Moreover, general metal contamination in nesting females' green sea turtles has been negatively correlated with omega-3 fatty acid levels in egg yolks—nutrients essential for proper embryonic development—suggesting a potential disruptive influence of these metals in embryo development by altering the composition of these crucial nutrients (Morão et al., 2024). However, more research is needed to better understand the consequences of contaminants on the reproductive success and survival of sea turtles, especially for vulnerable populations as it is the case of hawksbill sea turtles from São Tomé Island (Ferreira et al., 2018; Ferreira-Airaud et al., 2022). Closing this knowledge gap is essential for developing effective conservation strategies and ensuring the long-term viability of these endangered species.

Thus, to address these concerns, the main objectives of this study were to investigate: 1) the levels of metals and metalloids accumulated by nesting female of hawksbill sea turtles; 2) possible genotoxic effects of these elements in the blood of nesting females; 3) potential effects of these elements on their eggs in terms of morphometric characteristics and on the quality of their essential lipidic reserves for embryo development (fatty acids in the yolk).

## 2. Material and methods

This work with hawksbill sea turtles was ethically approved and the samples were imported to Portugal (Polytechnic of Leiria) under CITES permission (18ST000002/AC, 18PTLX00158I) issued by the "Direção Geral do Ambiente (DGA)" of São Tomé and Príncipe (STP) and the "Instituto da Conservação da Natureza e das Florestas (ICNF)" of Portugal.

### 2.1. Sampling site and data collection

The São Tomé and Príncipe archipelago is a small island nation located off the Central West Coast of Africa (0.263584° N, 6.602234° E). It consists of two equatorial oceanic islands, São Tomé (857 km<sup>2</sup>) and Príncipe (139 km<sup>2</sup>), along with several smaller islets, including Rolas islet (−0.006874° N, 6.522882° E) (Ceríaco et al., 2022). Situated in the southern part of São Tomé, Rolas islet (see Fig. 1) is a small rocky islet (~2 km off the southern tip of São Tomé) characterized by a tropical climate and abundant biodiversity, which spans both marine and terrestrial ecosystems. This islet is particularly notable as the primary nesting site for hawksbill turtles within the archipelago (Ferreira-Airaud et al., 2024), and it was in this Islet that the sampling for the present study took place (Fig. 1).

While this islet itself has limited agricultural activity due to its small size, its location in the southern region of São Tomé places it near potential contamination sources described in the introduction. The proximity to the mainland, where agriculture (e.g., oil palm, cassava, and cocoa plantations) and urban runoff contribute to metal contamination,



Fig. 1. Geographical localization of Rolas Islet (São Tomé and Príncipe archipelago) in relation to Africa, indicating the hawksbill sea turtle sampling site.

suggests that environmental pollutants could still reach the islet.

Blood samples from 12 hawksbill sea turtle females were obtained from their dorsal cervical sinus using a 20 Gauge 0.9 × 40 mm needle and a 5 mL syringe during their nesting activities. During this period, the 12 nesting females were measured (curved carapace length: CCL; and curved carapace width: CCW) using a fiberglass measuring tape ( $\pm 0.1$  cm) and tagged if they had not been before marked. The collected blood was promptly transferred into 6 mL sterile Vacutest® blood collection tubes containing the anticoagulant dipotassium ethylenediaminetetraacetic acid ( $K_2EDTA$ ) for metal and metalloid analysis (Section 2.2). Simultaneously, during the blood collection, two blood smears per female were prepared using one drop of blood. Following the drying process, the smears were securely sealed with hair lacquer and stored for subsequent genotoxicity analysis (Section 2.3).

Additionally, the sampling included the collection of freshly laid eggs, with one egg collected randomly from each female. Strict measures were taken to ensure no contact with the surrounding sand during egg collection. The collected eggs were immediately placed in individual zip bags and stored at  $-20$  °C for subsequent morphometric measurements (Section 2.4) and lipid analysis (Section 2.5).

All samples were collected after the females had already laid approximately 20 eggs to minimize the risk of nest abandonment (Morão et al., 2022).

## 2.2. Metal and metalloid analysis and pollution load index (PLI)

A total of 13 chemical elements were quantified in the blood samples of adult female hawksbill turtles (Al, As, Pb, Cd, Cr, Fe, Cu, Mn, Ni, Hg, Se, Ag, Zn). Before proceeding with the element analysis, the blood samples were weighed and freeze-dried for 48 h. Subsequently, the dried samples (500 mg) were digested using a High-Performance Microwave Digestion System (ETHOS UP, Milestone Connect, USA) with a mixture of 8 mL of nitric acid ( $HNO_3$  65 %) and 2 mL of hydrogen peroxide ( $H_2O_2$  33 %), both of analytical grade (<99 % purity). Quality control was carried out with analytical blanks and the certified reference material (CRM) TORT-3 lobster hepatopancreas.

Metals and metalloids quantification was performed by Inductively Coupled Plasma Optical Emission Spectroscopy (ICP-OES), using an ICP-OES model Ultima (Horiba Jobin-Yvon, France). The instrument was operated following the manufacturer's recommended settings, with a radiofrequency power of 1.05 kW, a plasma gas flow rate of 12.0 L  $min^{-1}$ , and a nebulizer gas flow rate of 0.5 L  $min^{-1}$ . The analytical wavelengths (nm) and limits of detection of the method (LOD) for each element, along with corresponding calibration curves and correlation coefficients, as well as recovery percentages, can be seen in Table S1.2.1 (supplementary material). The limits of detection (LOD) of the method for each element were determined as the concentration equivalent to

three times the standard deviation of ten blank measurements ( $n = 10$ ), divided by the slope of the respective calibration curve. Control standards were analysed between sample batches to ensure instrument calibration remained stable, and the calibration curves with their respective correlation coefficients were continuously monitored.

Metal concentrations below the limits of detection were estimated and adjusted using the method proposed by Hites (2019). In this approach, the values were estimated by taking the mean value between zero and the LOD value (i.e., LOD/2), after converting the LOD from  $\mu\text{g}\cdot\text{L}^{-1}$  to  $\mu\text{g}\cdot\text{g}^{-1}$  (d.w.) taking into consideration the volume and weight of each specific digested sample. This correction method was applied to a maximum of two turtles per element: aluminum (one turtle), mercury (two turtles), manganese (one turtle), and lead (one turtle). Metal concentrations were expressed in  $\mu\text{g}\cdot\text{g}^{-1}$  of blood dry weight (d.w.).

To provide a more integrative assessment of the overall trace element contamination in hawksbill sea turtles' blood, a Pollution Load Index (PLI) was calculated following Tomlinson et al. (1980), employing a normalization approach using Concentration Factors (CF) for individual elements (C metal) detected in the turtles' blood. Reference values from captive hawksbill sea turtles (Suzuki et al., 2012) served as the baseline concentration (C baseline) for all analysed elements, a methodology previously employed in other studies (Angulo, 1996; Morão et al., 2024). By using CF rather than absolute concentrations, this method accounts for natural background levels of both essential and non-essential elements, preventing potential overestimation due to the inclusion of biologically important metals. The resulting PLI thus offers a standardized metric to compare contamination levels relative to the reference group. The equations applied were as follows:

$$CF = \frac{C \text{ metal}}{C \text{ baseline}} \quad (1)$$

$$PLI = \sqrt[n]{CF1 \times CF2 \times CF3 \times \dots \times CFn} \quad (2)$$

### 2.3. Genotoxicity biomarker

The blood smears, two per female, were stained with Diff-Quick stain. A total of 1000 mature erythrocytes were examined per female to assess erythrocytic nuclear abnormalities (ENA). The nuclear lesions were categorised and scored as micronuclei, lobed nuclei, segmented nuclei and kidney-shaped nuclei, as previously described by Morão et al. (2024) and Casini et al. (2018). The results were represented as the average value (%) of each abnormality (ENA frequency), as well as the total count of all observed lesions (Total ENA).

### 2.4. Egg morphometric characteristics

The eggs were carefully rinsed with deionized water (Milli-Q Millipore, Merck) and subsequently weighed ( $\pm 0.01$  g) and measured using a Vernier calliper (Avantor, 819-0012) for three consecutive measurements. Following this, each egg was divided into its components, including the shell, membrane, albumen and yolk, which were individually weighed ( $\pm 0.01$  g). The separation process was performed promptly and manually to prevent excessive thawing of the eggs as in Morão et al. (2024).

To measure the thickness of the eggshell, two separate incisions were made in different areas of the shell to ensure representative and accurate measurements. The handling and examination of the turtle eggshells were conducted using a trinocular stereo zoom microscope (ZEISS STEMI, 2000-C, Carl Zeiss MicroImaging GmbH, Göttingen, Germany) at either 4x or 3.2x magnification. Subsequently, image capture was conducted using the AxioCam MRc camera (Carl Zeiss Microscopy GmbH, Göttingen, Germany), and the Zen 2011 application (blue edition) software was employed for conducting measurements, with a scale of 200  $\mu\text{m}$ .

Afterwards, the egg yolks were homogenised and separated into

aliquots of 2 g for posterior lipid extraction, quantification, and fatty acid profiling (section 2.5).

### 2.5. Yolk lipid and fatty acid profile

Total lipids were extracted and quantified (gravimetrically) from the previously separated yolk samples following the established methodology of (Bligh and Dyer, 1959). Specifically, a volume of 9 mL of a methanol/chloroform mixture (2:1 v/v) was added to 2 g of the yolk.

Prior to the methylation process for the analysis of the fatty acid profile, a separation of polar and neutral lipids was performed using Thin Layer Chromatography (TLC) plates. To analyse more complex lipids such as phospholipids (PL), an initial step of alkaline hydrolysis (saponification) was performed to extract the polar fraction from the TLC plate for each sample. Subsequently, the fatty acid profile analysis was conducted using established methods, which were thoroughly described in Morão et al. (2024) and can be also found in section 1.1 of supplementary material (SM).

External standards of fatty acid methyl ester mixes, including PUFA No1 from a marine source, PUFA No3 from menhaden oil, and a 37-component FAME mix, were used (Supelco, Bellefonte, PA, USA). To ensure accurate fatty acid quantification, a theoretical correction factor (FCT) specific to the FID detectors was applied, following the methodology described by (Guo (2014)). The present work considered highly unsaturated fatty acids (HUFA) as fatty acids (FA) with four or more unsaturations in their aliphatic chain (Morão et al., 2024). Results are expressed as  $\text{mg}\cdot\text{g}^{-1}$  of total fatty acids.

### 2.6. Statistical analysis

Summary statistics included means, standard deviations (SD), and ranges (minimum-maximum) for each parameter. All statistical analyses used a significance level of 0.05. The Shapiro-Wilk test examined data normality (see Table S1.3.1 in SM). Differences between fractions, classes, and FA ratios were assessed using the Paired Samples *t*-test for samples exhibiting a normal distribution, while Wilcoxon test was used for non-normally distributed data.

Spearman's linear correlation coefficients (Evans, 1996) were used to examine the correlations between egg morphometric measurements and FA levels with metal concentrations and PLI index. Evans' guidelines (1996) were used to characterise correlation strength, by looking at the correlation coefficient as follows: "very weak" (0.00–0.19), "weak" (0.20–0.39), "moderate" (0.40–0.59), "strong" (0.60–0.79), and "very strong" (0.80–1.0).

Canonical Correspondence Analysis (CCA) was employed to explore the distribution patterns and relationships among metal concentrations and fatty acid profile. Prior to this analysis, metals and metalloids data was standardised and log-transformed using the formula  $\log(x + 1)$  (Hsu and Culhane, 2020). Additionally, FA profile was downweighed to account for less representative FA (Lepš and Šmilauer, 2003).

Correlation analysis, paired samples *t*-tests and Wilcoxon tests were conducted using IBM SPSS Statistics 28.0.1.0 (IBM Corp, 2023). Canonical Correspondence Analysis (CCA) was carried out using CANOCO version 4.5 package 5 (ter Braak and Šmilauer, 2002).

## 3. Results

### 3.1. Trace element levels and pollution load index (PLI)

The results of metals and metalloids analysed in the blood of nesting hawksbill female sea turtles are presented in Table 1. The elements Ag, Cd, Cr, and Ni were below the limit of detection across all sampled individuals and were therefore omitted from further statistical analyses.

The highest levels among the metals were observed for Fe ( $120.01 \pm 32.60 \mu\text{g}\cdot\text{g}^{-1}$ ), followed by Zn ( $5.35 \pm 0.92 \mu\text{g}\cdot\text{g}^{-1}$ ) and Pb ( $0.18 \pm 0.03 \mu\text{g}\cdot\text{g}^{-1}$ ). Between the two metalloids, Se presented the highest

**Table 1**

Element concentrations ( $\mu\text{g}\cdot\text{g}^{-1}$ ), concentration factors (CF) for each element analysed and pollution load index (PLI) values for hawksbill sea turtles (*Eretmochelys imbricata*) calculated with reference values observed for captive turtles (Suzuki et al., 2012) as the baseline. Mean, standard deviation (SD), minimum, and maximum values for each parameter are presented. Al = aluminium, As = arsenic, Cu = cooper, Fe = iron, Hg = mercury, Mn = manganese, Pb = lead, Se = selenium and Zn = zinc.

		Elements concentration ( $\mu\text{g}\cdot\text{g}^{-1}$ )				Concentration Factor (CF)				Pollution Load Index (PLI)			
		Mean	SD	Min	Max	Mean	SD	Min	Max	Mean	SD	Min	Max
<b>Metals</b>	Al	0.06	0.04	0.02	0.14	0.05	0.03	0.01	0.13	9.3	4.05	2.55	18.7
	Cu	0.10	0.03	0.01	0.13	6.5	2.51	0.87	10.18				
	Fe	120.01	32.60	75.83	215.48	688.47	275.55	428.34	1526.92				
	Pb	0.07	0.04	0.01	0.19	1.08	0.84	0.1	3.5				
	Mn	0.02	0.01	0.00	0.02	2.61	1.17	0.02	4.37				
	Hg	0.18	0.03	0.15	0.22	5.27	1.42	3.63	8.16				
	Zn	5.35	0.92	4.52	7.92	30.49	9.4	21.17	55.73				
<b>Metalloids</b>	As	0.46	0.44	0.07	1.69	90.84	86.82	13.76	303.08				
	Se	6.19	6.28	1.01	17.00	202.35	218.84	29.05	665.6				

concentration ( $6.19 \pm 6.28 \mu\text{g}\cdot\text{g}^{-1}$ ) and As a lower concentration ( $0.46 \pm 0.44 \mu\text{g}\cdot\text{g}^{-1}$ ).

The analysis of concentration factors (CF; Table 1 and Table S2.1.1) for each element indicated that the metal Fe exhibited the highest values ( $688.47 \pm 275.55$ ), followed by the metalloids Se ( $202.35 \pm 218.84$ ) and As ( $90.84 \pm 86.82$ ), and by the metal Zn ( $30.49 \pm 9.40$ ). On the other hand, the metal Al showed the lowest CF value ( $0.05 \pm 0.03$ ). The overall PLI for the sampled hawksbill sea turtles was  $9.30 \pm 4.05$ , with a minimum value of 2.55 and a maximum of 18.70 (Table 1).

### 3.2. Genotoxicity effects

The frequencies of nuclear abnormalities in hawksbill sea turtles' erythrocytes are summarised in Table S2.2.1 (SM). Fig. 2 presents a photomicrographic representation of erythrocytic nuclear abnormalities.

Lobed nuclei presented the highest mean frequency of  $72.50 \% \pm 37.58$ , followed by kidney-shaped nuclei with a mean frequency of  $4.50 \% \pm 3.50$  and segmented nuclei with  $0.25 \% \pm 0.60$  frequency. Micronuclei had a mean frequency of  $0.17 \% \pm 0.37$  and the frequency of Total ENAs was  $77.42 \% \pm 37.60$  (Table S2.2.1).

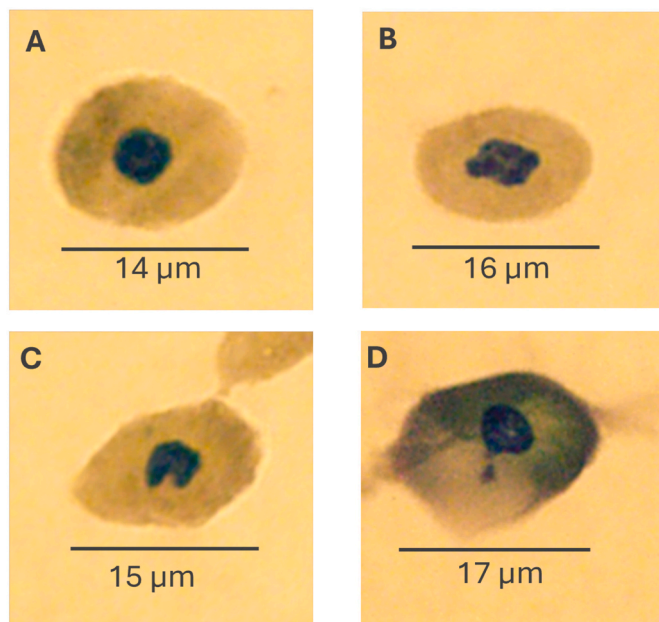


**Fig. 2.** Photomicrographic representation of erythrocytic nuclear abnormalities observed in the blood of hawksbill sea turtle (*Eretmochelys imbricata*). A = normal cell; B = lobed-shaped nucleus; C = kidney-shaped nucleus; D = micronucleus.

When analysing the correlations between the metal and metalloids levels and the different ENA observed, a positive correlation was found between Hg levels and lobed nuclei ( $r_s = 0.61$ ;  $p = 0.03$ ; Table S2.2.2). On the other hand, higher levels of the overall elements (PLI) were associated with decreased segmented nuclei ( $r_s = -0.65$ ;  $p = 0.02$ ), particularly for As ( $r_s = -0.65$ ;  $p = 0.02$ ), Mn ( $r_s = -0.59$ ;  $p = 0.04$ ) and Se ( $r_s = -0.64$ ;  $p = 0.03$ ) (details in Table S2.2.2).

### 3.3. Egg morphometric measurements and lipid content

The size measurements of the nesting females (CCL and CCW) are provided in the supplementary material (see Table S2.3.1). The analysis of their relationship with egg diameter revealed no significant correlations ( $p > 0.05$ ).

The morphometry of the sampled eggs is described in Table 2. The egg yolk, with  $9.67 \pm 1.05$  g, represented almost half of total egg weight ( $19.95 \pm 1.62$  g), with Total Fat (TF) accounting for around 11 % of the total yolk weight.

Saturated fatty acids (SFA) presented the highest percentage in egg yolks, followed by monounsaturated (MUFA), highly unsaturated (HUFA) and polyunsaturated (PUFA) (Table 3). The Triacylglycerols (TAG) and Cholesteryl Esters (CE) classes, pooled and considered here as Neutral Fraction (NF), is composed of similar percentages of SFA (48.11 %) and MUFA (47.89 %), followed by HUFA (2.76 %) and PUFA (1.25 %). The phospholipids fraction, designated here as Polar Fraction (PF), is mainly composed of SFA (52.75 %) followed by MUFA (30.54 %), HUFA (15.11 %) and PUFA (1.60 %). The NF exhibited a notably higher percentage of MUFA compared to the PF (Table 3,  $p < 0.001$ ). Conversely, the PF showed a significantly higher percentage of HUFA compared to the NF (Table 3,  $p < 0.001$ ). SFA and PUFA classes presented similar levels across the two lipid fractions.

The disparity in MUFA can be attributed to the higher percentage of omega-7 (n7) and omega-9 (n9) fatty acids groups in NF, while the differences in HUFA are due to the higher percentage of omega-3 (n3) and omega-6 (n6) fatty acids in PF. Accordingly, the percentage of n3 and n6 fatty acids was significantly higher in the PF than in the NF

**Table 2**

Mean  $\pm$  standard deviation and range values (minimum-maximum) for morphometric characteristics of the nesting *Eretmochelys imbricata* eggs ( $n = 12$ ).

Morphometric characteristics	Average $\pm$ SD (min – max)
Diameter (mm $\pm$ 0.01)	32.57 $\pm$ 1.34 (30.07–34.20)
Whole egg (g)	19.95 $\pm$ 1.62 (17.32–23.33)
Shell thickness ( $\mu\text{m}$ )	136.54 $\pm$ 18.37 (110.76–170.41)
Yolk (g)	9.67 $\pm$ 1.05 (8.40–11.91)
Shell (g)	1.66 $\pm$ 0.28 (1.27–2.16)
Albumin (g)	5.32 $\pm$ 1.08 (3.23–6.82)
Membrane (g)	2.08 $\pm$ 0.30 (1.46–2.54)
Yolk Total Fat (%)	11.40 $\pm$ 2.40 (7.10–14.07)

**Table 3**

Composition of various fatty acid categories (mean  $\pm$  standard deviation; mg. g<sup>-1</sup> Total FAs) and key fatty acid content ratios in *Eretmochelys imbricata* egg yolk samples in both Neutral (NF) and Polar (PF) fractions. SFA = saturated fatty acids; MUFA = monounsaturated fatty acids; PUFA = polyunsaturated fatty acids; HUFA = highly unsaturated fatty acids; DHA = docosahexaenoic acid; EPA = eicosapentaenoic acid. \* = statistical differences between fractions using Paired samples *t*-test (a) or Wilcoxon test (b).

FA categories	Neutral Fraction (NF)	Polar Fraction (PF)	Significance values (p)
SFA	48.11 $\pm$ 1.43*	52.75 $\pm$ 0.89*	0.028 (a)
MUFA	47.89 $\pm$ 1.42*	30.54 $\pm$ 0.52*	<0.001 (a)
PUFA	1.25 $\pm$ 0.04*	1.60 $\pm$ 0.03*	0.023 (b)
HUFA	2.76 $\pm$ 0.08*	15.11 $\pm$ 0.26*	<0.001 (a)
n3	1.62 $\pm$ 0.05*	7.68 $\pm$ 0.13*	<0.001 (a)
n6	1.80 $\pm$ 0.05*	8.41 $\pm$ 0.14*	0.002 (b)
n7	13.68 $\pm$ 0.41*	3.86 $\pm$ 0.07*	<0.001 (a)
n9	33.19 $\pm$ 0.98*	23.62 $\pm$ 0.40*	<0.001 (a)
trans	1.41 $\pm$ 0.04*	2.12 $\pm$ 0.04*	0.001 (a)
n3/n6	0.93 $\pm$ 0.35	0.96 $\pm$ 0.35	0.717 (a)
DHA/EPA	1.74 $\pm$ 1.07	1.27 $\pm$ 0.41	0.117 (b)
SFA/UNSAT	0.93 $\pm$ 0.07*	1.14 $\pm$ 0.23*	0.004 (b)
SFA/PUFA	44.28 $\pm$ 14.54*	33.60 $\pm$ 5.44*	0.021 (a)
SFA/HUFA	21.32 $\pm$ 9.85*	3.72 $\pm$ 1.01*	<0.001 (a)
MUFA/PUFA	45.05 $\pm$ 17.31*	19.64 $\pm$ 3.80*	<0.001 (a)
MUFA/HUFA	21.73 $\pm$ 11.21*	11.21 $\pm$ 2.16*	<0.001 (a)

(Table 3,  $p < 0.001$ ). Conversely, for n7 and n9 groups, the NF significantly exhibited higher percentages than the PF (Table 3,  $p < 0.001$ ).

Regarding differences in important ratios between the two fractions, SFA/HUFA, MUFA/PUFA and MUFA/HUFA presented higher and significant values in NF (Table 3,  $p < 0.001$  and  $p = 0.002$  respectively). The ratios n3/n6 and DHA/EPA presented similar values in the two fractions ( $p = 0.717$  and  $p = 0.117$ , respectively) and the ratio SFA/UNSAT exhibited higher levels in PF ( $p = 0.004$ ).

Overall, the yolk samples exhibited fatty acids (FAs) ranging from 6:0 (caproic acid) to 24:1 n9 (nervonic acid), containing a comprehensive total of 48 distinct FAs identified and detected across this study (Table S2.3.2, SM). The predominant FAs in hawksbill sea turtle yolk samples within the NF were 18:1n-9 (oleic acid, 304.37  $\pm$  36.45 mg g<sup>-1</sup>), 16:0 (palmitic acid, 247.18  $\pm$  18.08 mg g<sup>-1</sup>), 14:0 (myristic acid, 142.55  $\pm$  13.91 mg g<sup>-1</sup>), 16:1n-7 (palmitoleic acid, 92.75  $\pm$  15.67 mg g<sup>-1</sup>), followed by the similar amounts of 18:1 n-7 (vaccenic acid, 36.36  $\pm$  6.58 mg g<sup>-1</sup>) and 18:0 (stearic acid, 36.31  $\pm$  6.34 mg g<sup>-1</sup>) (Table S2.3.2). Conversely, within the PF, the major FAs were 16:0 (palmitic acid, 225.73  $\pm$  26.44 mg g<sup>-1</sup>), 18:1n-9 (oleic acid, 212.39  $\pm$  20.87 mg g<sup>-1</sup>), 18:0 (stearic acid, 184.72  $\pm$  28.30 mg g<sup>-1</sup>), 20:4 n-6 (arachidonic acid, ARA, 70.18  $\pm$  19.83 mg g<sup>-1</sup>), 12:0 (lauric acid, 37.90  $\pm$  11.27 mg g<sup>-1</sup>) and 14:0 (myristic acid, 30.37  $\pm$  5.15 mg g<sup>-1</sup>). Notably, the major FAs present in both fractions were 18:1n-9, 18:0, 16:0 and 14:0. However, the PF also exhibited noteworthy amounts of other crucial fatty acids, such as 20:5 n-3 (eicosapentaenoic acid, EPA, 22.18  $\pm$  9.92 mg g<sup>-1</sup>) and 22:6 n-3 (Docosahexaenoic acid, DHA, 27.46  $\pm$  12.88 mg g<sup>-1</sup>). This demonstrates a considerable variation in concentrations, ranging from 0.02 to 225.73 mg g<sup>-1</sup>, across all the analysed fatty acids (Table S2.3.2).

### 3.4. Blood trace element concentrations versus egg morphometric characteristics

No significant correlations were registered between the analysed egg morphometric parameters and the pollution load index (PLI) (Table S2.4.1, SM). However, strong positive correlations between Se levels and both eggshell weight ( $r_s = 0.69$ ;  $p = 0.01$ ) and eggshell thickness ( $r_s = 0.69$ ;  $p = 0.01$ ) were found (Table S2.4.1). Al levels also showed a strong significant and positive correlation with the egg's membrane weight ( $r_s = 0.62$ ;  $p = 0.03$ ; Table S2.4.1). On the contrary,

strong negative correlations were verified between Pb levels and the diameter of their eggs ( $r_s = -0.66$ ;  $p = 0.02$ ; Table S2.4.1).

### 3.5. Blood trace element concentrations versus yolk fatty acids

To assess the possible interaction between environmental contaminants found in females' blood and the fatty acid profile in their egg yolk samples, a Canonical Correspondence Analysis (CCA) was conducted separately for each yolk fraction (Fig. 3). This analysis was performed to assess relationships with classes of FAs (Fig. 3A and C) and individual FAs (Fig. 3B and D).

When analysing the influence of metals and metalloids on the distribution of fatty acid classes, a different pattern is observed in the two fractions (NF and PF). The initial two CCA components of the NF for FA classes (Fig. 3A) account for 99.6 % of the variability associated with females' contamination. A negative association can be observed between the levels of Zn, Fe, Cu, Mn, and Pb and the distribution of MUFA and SFA fatty acids, while a positive association is noted between Zn and Pb with PUFA (Fig. 3A). Conversely, these PUFA appear to be negatively influenced by Se and Al. Additionally, Fe, Cu, and Mn are associated with HUFA in a positive manner. Regarding PF (Fig. 3C), the initial two components of the CCA for FA classes explain 95.30 % of the variability linked to contaminant load. Here, it is more evident that the presence of metals and metalloids in general have a remarkably negative influence on SFA and PUFA fatty acids. Additionally, it is observed a positive influence from the levels of Mn, Hg, Zn, Pb, Cu, and Fe on HUFA fatty acids (Fig. 3C).

When analysing the influence of metals on the levels of individual fatty acids, more detailed responses can be observed (Fig. 3B and D). In the NF (Fig. 3B), most fatty acids are concentrated in the centre of the biplot, indicating a lesser influence of the metals on these fatty acids (51.7 % explanation by the two components of the biplot). In the PF (Fig. 3D), a similar central cluster of fatty acids is observed in the biplot but there is a higher degree of dispersion of the fatty acids, indicating a greater influence of metals in this yolk fraction (53.8 % explanation by the two components of the biplot). In the NF, Se is seen as one of the elements contributing more for the variability of the FA data (Fig. 3B), which is corroborated by the correlation analyses that showed a higher number of significant correlations, both negative and positive, with Se (Table S2.5.1, SM). The negative and significant correlations were mostly with SFA fatty acids such as 16:0 (Palmitic acid;  $r_s = -0.62$ ;  $p = 0.03$ ), 18:0 (Stearic acid;  $r_s = -0.78$ ;  $p < 0.001$ ) and 20:0 (Arachidic acid;  $r_s = -0.59$ ;  $p = 0.04$ ) (Fig. 3B and Table S2.5.1). Conversely, essential metals Cu and Fe presented positive and significant correlations with n-6 fatty acids ( $r_s = -0.60$ ;  $p = 0.04$  and  $r_s = -0.66$ ;  $p = 0.02$ , respectively) namely with 20:4 n-6 (Arachidonic acid; ARA;  $r_s = -0.62$ ;  $p = 0.03$  and  $r_s = -0.66$ ;  $p = 0.02$ , respectively) and 22:3 n-6 (Docosatraenoic acid; DHA;  $r_s = -0.62$ ;  $p = 0.03$  and  $r_s = -0.77$ ;  $p < 0.001$ , respectively) (Fig. 3B and Table S2.5.1).

For PF, a different dispersion pattern was observed and the overall analysis revealed that non-essential metals, specifically Al, As, and Hg, had the most substantial influence and displayed the highest negative correlations with FAs (Fig. 3D and Table S2.5.2 in SM). Notably, and despite the overall trend of a negative influence of the analysed metals in total FAs (except for Mn and Zn), As even exhibited a significant negative correlation with the total amount of FAs ( $r_s = -0.66$ ;  $p = 0.02$ ). Contrarily to the other elements, Se was the only one presenting exclusively positive correlations (Table S2.5.2). Moreover, the overall contamination index (PLI) was negatively correlated with the SFA fatty acids in the PF ( $r_s = -0.69$ ;  $p = 0.01$ , Table S2.5.2), especially justified by the negative correlations of Al and Cu with this fatty acid class ( $r_s = -0.62$ ;  $p = 0.03$  and  $r_s = -0.64$ ;  $p = 0.02$ , respectively) (Fig. 3D and Table S2.5.2). Despite non-significant, the same negative trend was observed for the other metals analysed (Table S2.5.2). Among these SFA fatty acids, 16:0 (palmitic acid) presented the highest strong negative correlations with Al ( $r_s = -0.85$ ;  $p < 0.001$ ) and Cu ( $r_s = -0.67$ ;  $p =$

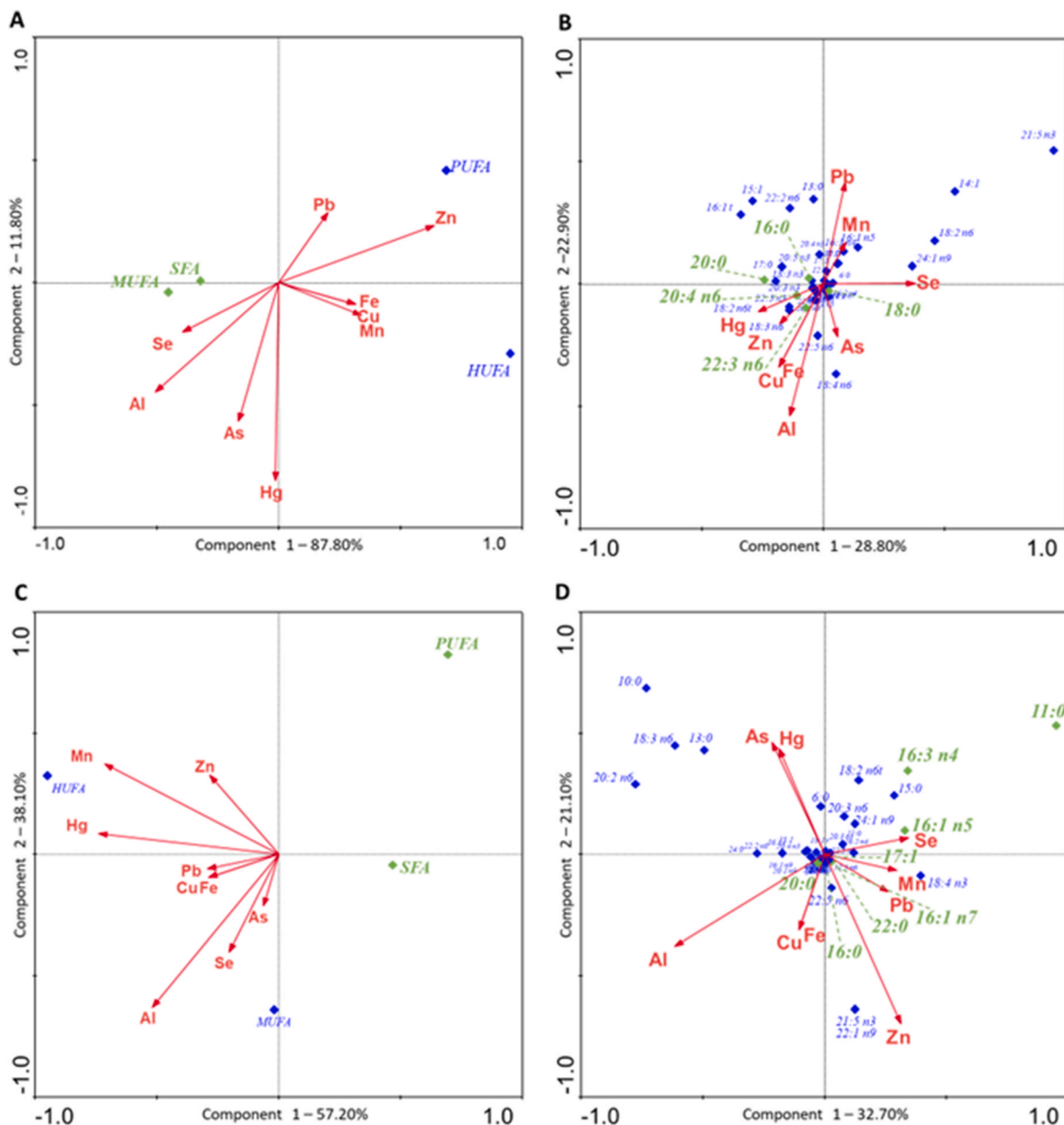


**Fig. 3.** Biplots for axes 1 and 2 of the Canonical Correspondence Analysis (CCA) between the metal levels in the blood of female *Eretmochelys imbricata* and the fatty acid (FA) profile in their egg yolk samples, in relation to FA classes (A, C) and individual FAs (B, D) of the neutral (A and B) and the polar (C and D) fractions of the yolk samples. Red arrows indicate metals, blue or green diamonds represent FA classes in A and C, and individual FAs in B and D. The most representative fatty acids are highlighted in green. (The green dashed lines are not vectors and are not part of the analysis. They are solely provided as a visual aid to improve readability of the data).

0.02) (Table S2.5.2). The same negative trend was generally observed for other longer chain SFAs (20:0 and 22:0). Furthermore, Se was the only element showing positive correlations with metabolically important FAs, namely with MUFA ( $r_s = 0.66$ ;  $p = 0.02$ ), n-7 ( $r_s = 0.66$ ;  $p = 0.02$ ) and n-9 ( $r_s = 0.59$ ;  $p = 0.04$ ) groups (Table S2.5.2). Specifically, this essential metal exhibited a positive correlation with FAs such as 16:1 n7 (palmitoleic acid;  $r_s = 0.75$ ;  $p = 0.01$ ) and its isomer (16:1 n5 ( $r_s = 0.72$ ;  $p = 0.01$ ) and 17:1 (heptadecenoic;  $r_s = 0.85$ ;  $p < 0.001$ ). In contrast, the essential metal Zn had the most significant negative correlations with 11:0 (undecanoic acid;  $r_s = -0.78$ ;  $p < 0.001$ ) and 16:3 n4 (palmitolenic acid;  $r_s = -0.59$ ;  $p = 0.04$ ) (Fig. 3D and Table S2.5.2).

#### 4. Discussion

To the best of our knowledge, this study represents the first

comprehensive report on metal contamination in the critically endangered hawksbill sea turtles nesting in São Tomé Island and in Gulf of Guinea region. This work provides valuable information regarding metal contamination load in females, the possible genotoxic effects in females' erythrocytes and intricate relationship between metal contamination load with morphology, lipid reserves and fatty acid profile in their fresh laid eggs.

##### 4.1. Contaminant levels in females' blood

Sea turtles are susceptible to accumulate metals in their tissues, depending on their feeding habits. Those that feed at higher trophic levels have more propensity to bioaccumulate these contaminants, compared to species that feed at lower trophic levels (Ross et al., 2017). This accumulation may have consequences for their health and for their

future generations (Day et al., 2007; Perrault et al., 2011).

Given their dietary differences, it was hypothesized that hawksbill sea turtles from the present study would show higher levels of metals and metalloids compared to the green sea turtles from the same area, as previously analysed (see Table 4, Morão et al., 2022, 2024). While both species share an omnivorous diet during their juvenile stages, green sea turtles shift to their herbivorous feeding in adulthood, whereas hawksbills tend to adopt a more carnivorous diet, feeding mostly on sponges (Baumbach et al., 2022; Jones and Seminoff, 2013). However, only the levels of Hg and Se were higher in hawksbill's blood compared to green sea turtles (Table 4). These two elements are known to interact, as Se has been shown to reduce the toxicity of Hg (Chen et al., 2006). Interestingly, the levels of circulating Se were notably higher than those of Hg in the blood of both sea turtle species from São Tomé Island, with Se/Hg molar ratios above 100 for both species, suggesting that Se may be contributing to reduce the bioavailability and toxicity of Hg in the blood of these female turtles.

While these findings may seem predictable given the differences in feeding habits and metabolism between the species, higher Hg levels observed in hawksbill turtles - despite other metals being more abundant in green sea turtles - could point to potential differences in the accumulation dynamics of Hg in the blood between species. In fact, erythrocytes are a primary target for Hg, due to the metal's strong affinity for the thiol groups in glutathione (GSH), which is found in high concentrations in erythrocytes for detoxification purposes (Bridges and Zalups, 2017). Despite having lower overall contamination levels, hawksbill sea turtles may exhibit different accumulation dynamics for Hg, potentially due to variations in their metabolism or excretion mechanisms.

Observations from the local Non-Governmental Organization (NGO) Programa Tatô suggest that hawksbill sea turtles do not feed during nesting activities (Ferreira-Airaud et al., 2024), as observed in previous studies on this and other sea turtle species (Miller, 1997; Muñoz and Vermeiren, 2023). However, Programa Tatô NGO records indicate that some green sea turtles can actively feed during this nesting period (Ferreira-Airaud et al., 2024).

This difference in feeding behaviour, combined with the potential exposure to contaminants in distinct feeding areas, could explain the higher general levels of metals in green sea turtles compared with the levels present in hawksbill sea turtles from São Tomé Island. Moreover, considering that blood samples reflect recent exposure to contaminants over 2–3 weeks to 1–3 months depending on the element and its

speciation (Akinleye et al., 2024; Martinez-Morata et al., 2023; Shaw et al., 2021), these temporal and spatial differences may further influence the observed contamination patterns.

The overall lower contamination of the hawksbill sea turtles (except for Hg and Se) is also evident when comparing the Pollution Load index (PLI) values between species (see Table S3.1 in SM). The PLI values for the green sea turtles of the same geographical area has been previously determined in Morão et al. (2024). However, as the PLI calculation used reference values specific to green turtles, these differed from the reference values used in the present work. To enable direct comparison, data normalization using the same reference values was necessary to calculate the Concentration Factors (CFs), in this case the ones from captive hawksbill sea turtles (Suzuki et al., 2012). The recalculated PLI values revealed that, among the metals and metalloids commonly accumulated by both species, green sea turtles exhibited a higher PLI ( $32.26 \pm 12.12$ ) compared to hawksbills, whose PLI was  $9.30 \pm 4.05$ .

This finding aligns with previous observations that hawksbills generally show lower metal contamination levels, with the exceptions of Hg and Se (see Table S3.1 in SM). According to the classification of Goher et al. (2014), both hawksbill and green turtles could be facing a high risk of metal contamination, although the criteria was developed for water contamination. In contrast, the classification of Angulo (1996) for marine mussels suggests a relatively lower risk, as only PLI values above 50 indicate potential concern. However, since no established risk classification currently exists for sea turtles or other higher vertebrates, future studies are critical to better understand the link between PLI values and actual biological impacts in these species. Additionally, developing a standardized classification system specific to marine turtles, taking into account species-specific and life-stage differences, would enhance long-term monitoring efforts for these endangered populations, providing valuable guidance for conservation and management strategies. Furthermore, it is important to consider that in nesting female turtles, the maternal transfer of trace elements during egg formation may influence blood metal concentrations at the time of sampling. This highlights the need for monitoring metal accumulation across different life stages to gain a more comprehensive understanding of exposure and potential risks over an individual's lifetime.

When comparing the present results with available studies in the literature on blood element levels (dry weight basis; Table 4), the values for the hawksbills from São Tomé were generally lower (except for Hg which showed similar values) than those reported for hawksbills from

**Table 4**

Metal concentrations (mean  $\pm$  standard deviation), determined in the blood of different species of adult female sea turtles ( $\mu\text{g}\cdot\text{g}^{-1}$  of d.w.). N = number of animals investigated; <LOD = below limit of detection; <LOQ = below limit of quantification. ICP-EAS = Inductively Coupled Plasma Atomic Emission Spectroscopy; AAS = Atomic Absorption Spectrophotometer; ICP-MS = Inductively Coupled Plasma Mass Spectrometry; FAAS = Flame Atomic Absorption Spectrophotometry; GFAAS = Graphite Furnace Atomic Absorption Spectrophotometry; (-) = Not Reported.

Species	<i>Eretmochelys imbricata</i>		<i>Chelonia mydas</i>	<i>Lepidochelys olivacea</i>		<i>Dermochelys coriacea</i>
	N	12	12	27	25	78
Localization	STP (Equatorial Atlantic)	Iran (Caspian Sea)	STP (Equatorial Atlantic)	Mexico (North Pacific)		French Guiana (North Atlantic)
<b>Metals</b>	Aluminium (Al)	0.06 $\pm$ 0.04	–	5.03 $\pm$ 20.78	–	–
	Cadmium (Cd)	<LOD	0.34 $\pm$ 0.08	0.03 $\pm$ 0.06	0.45 $\pm$ 0.20	–
	Chromium (Cr)	<LOD	–	0.02 $\pm$ 0.04	–	0.41 $\pm$ 0.15
	Copper (Cu)	0.07 $\pm$ 0.04	1.89 $\pm$ 0.78	3.79 $\pm$ 1.22	2.28 $\pm$ 0.40	–
	Iron (Fe)	120.01 $\pm$ 32.61	–	2189.59 $\pm$ 869.04	–	6.83 $\pm$ 1.43
	Lead (Pb)	0.18 $\pm$ 0.03	0.56 $\pm$ 0.25	0.97 $\pm$ 0.59	–	0.92 $\pm$ 0.26
	Manganese (Mn)	0.02 $\pm$ 0.01	–	0.78 $\pm$ 1.76	0.95 $\pm$ 0.18	–
	Mercury (Hg)	0.10 $\pm$ 0.03	0.18 $\pm$ 0.05	0.006 $\pm$ 0.012	–	0.06 $\pm$ 0.02
	Nickel (Ni)	<LOD	–	<LOQ	2.8 $\pm$ 1.3	–
	Silver (Ag)	<LOD	–	<LOQ	–	–
	Zinc (Zn)	5.35 $\pm$ 0.92	37.6 $\pm$ 3.98	91.30 $\pm$ 57.18	58.4 $\pm$ 4.7	56.61 $\pm$ 1.43
<b>Metalloids</b>	Arsenic (As)	0.46 $\pm$ 0.44	–	2.07 $\pm$ 1.59	–	–
	Selenium (Se)	6.19 $\pm$ 6.28	–	3.94 $\pm$ 4.48	–	50.9 $\pm$ 0.26
<b>Analytic system</b>	ICP-EAS	AAS	ICP-MS	FAAS and GFAAS	ICP-MS	ICP-MS
<b>Reference</b>	Present study	Ehsanpour et al. (2014)	Morão et al. (2022)	Páez-Osuna et al., 2010a	Páez-Osuna et al., 2010b	Guirlet et al. (2008)

Arabic Sea (Ehsanpour et al., 2014). In contrast, hawksbill sea turtles from São Tomé exhibited higher Hg levels than leatherback sea turtles (*Dermodochelys coriacea*) from French Guiana (Guirlet et al., 2008). Additionally, the present results indicated lower levels of Cu, Zn and Pb compared to those observed in leatherbacks from French Guiana (Guirlet et al., 2008) and olive ridleys from Gulf of Mexico (Páez-Osuna et al., 2010b, 2010a, Table 4). While differences in feeding habits among species may partly explain these variations, the contrasting metal accumulation levels could also be attributed to differences in contamination levels in their respective diets at each geographical location.

To mitigate the risks associated with metal contamination, it is essential to identify potential sources of Hg and other metals, whether from industrial or agricultural activities near São Tomé Island or in the turtles' foraging areas. This would allow for the implementation of stricter regulations on contaminant emissions, both locally and through collaboration with other countries where these turtles nest and may also be exposed.

#### 4.2. Genotoxicity in female erythrocytes

Despite the lack of information and reference values existing in the literature concerning total erythrocytic nuclear abnormalities (ENA) and even micronuclei (MN) count in hawksbill sea turtles, the findings of the current study indicated lower levels of MN ( $0.17\% \pm 0.37$ ) compared to our previous study on green sea turtles nesting in São Tomé Island (Morão et al., 2022), which reported an average of  $8.44 \pm 5.22$  micronuclei per 1000 counted erythrocytes. Moreover, these levels were lower compared to other populations of green sea turtles, including those from Mexico (average  $1.30\% \pm 2.32$ ) (Guevara-Meléndez et al., 2023), Brazil (average  $1.01\% \pm 0.69$ ) (da Silva et al., 2016), and loggerhead sea turtles from the Mediterranean Sea (average  $15.82\% \pm 15.16$ ) (Casini et al., 2018). Nonetheless, reference values for micronuclei have been established for freshwater turtles, with a baseline frequency of  $3.56\% \pm 1.39$  (Latorre et al., 2015), and for lizards, with a baseline frequency of  $0.95\% \pm 0.27$  (Schaumburg et al., 2012). In addition, for juvenile green sea turtles, a median baseline reference of 0 micronuclei and 2 nuclear buds per 1000 erythrocytes have been indicated (Labrada-Martagón et al., 2019). Present results fall within these established thresholds, suggesting probable low genotoxic effects in the hawksbill sea turtles from this study in terms of micronuclei formation.

Analyzing the other types of nuclear abnormalities, the hawksbill sea turtles in the present study exhibited higher values for lobed, kidney-shape, segmented nuclei and total ENA compared to green sea turtles from São Tomé and Príncipe (lobed  $19.08\% \pm 14.03$ ; kidney  $0.50\% \pm 0.69$ ; segmented  $0.08\% \pm 0.27$  and Total ENA  $28.31\% \pm 16.07$ ) (Morão et al., 2024) and higher values of total ENA than those of green sea turtles from Mexico ( $18.56\% \pm 32.89$ ; Guevara-Meléndez et al., 2023). In addition, the values for kidney and segmented nuclei were higher compared to those of loggerhead turtles from the Mediterranean Sea (kidney  $1\% \pm 1.91$ ; segmented  $0.08\% \pm 0.28$ , respectively), although lobed and total ENA values were lower compared to the same loggerheads (lobed  $207.97\% \pm 107.42$ ; and total ENA  $224.87\% \pm 111.34$ ) (Casini et al., 2018).

Moreover, when comparing the median values observed for green sea turtles (Labrada-Martagón et al., 2019) for nuclear buds, present median values for kidney (4.5) and lobed (56) shaped nuclei were higher than those reference values. Overall, these results suggest that the hawksbill turtles analysed in the present study show genotoxicity levels higher than the average observed for green sea turtles of the available studies but lower than the loggerheads from the Mediterranean Sea (Casini et al., 2018). This difference is likely to the high anthropogenic pressures experienced in the Mediterranean Sea, including intense shipping rates, domestic and industrial sewage, agricultural activities, commercial and touristic harbours, representing a critical input area for contaminants (Casini et al., 2018). Consequently, sea turtles inhabiting

this region are subjected to a higher concentration of genotoxic agents compared to hawksbills from São Tomé Island.

The formation of nuclear abnormalities such as lobed nuclei may arise from chromosomal attachment issues or gene amplification through the Breakage-Fusion-Bridge (BFB) cycle, as cells attempt to eliminate excess amplified DNA from the nucleus (Ergene et al., 2007). Segmented nuclei, on the other hand, are linked to challenges during cell division, such as improper spindle formation, which results in genetic material being erratically distributed (Amorim et al., 2024). While these abnormalities provide insights into cellular disruptions, their interpretation remains controversial, with some authors suggesting they indicate cytotoxicity rather than genotoxicity (Canedo et al., 2021; Castro et al., 2018).

Interestingly, the current findings reveal a significant negative correlation between general contamination (PLI) ( $r_s = -0.65$ ;  $p = 0.02$ ) and segmented nuclear abnormalities. Particularly, with As ( $r_s = -0.65$ ;  $p = 0.02$ ), Mn ( $r_s = -0.59$ ;  $p = 0.04$ ) and Se ( $r_s = -0.64$ ;  $p = 0.03$ ) emerging as the metals most closely linked to this association. However, it is important to note that only two out of the twelve hawksbill turtles analysed exhibited segmented nuclear abnormalities, which limits the representativeness and robustness of these observations, suggesting that the results may not reflect a generalizable trend. Thus, these associations should be interpreted with caution and future research with larger and more representative samples is needed to validate and better understand these potential interactions and their effects on segmented nuclear abnormalities.

Conversely, a strong positive correlation was observed between Hg levels and the occurrence of lobed-shaped nuclei ( $r_s = 0.61$ ;  $p = 0.03$ ), similar to findings in previous studies with green sea turtles (Morão et al., 2024). This supports the idea that mercury interacts with erythrocytes leading to specific nuclear abnormalities. Mercury's preferential accumulation in erythrocytes has been documented to cause morphological and functional changes, including disruptions in oxygen transport, ion exchange and antioxidant balance, leading to lipid damage and membrane deformation (Bridges and Zalups, 2017; Piscopo et al., 2020; Shalan, 2022).

These impacts are further supported by studies showing genotoxicity effects of Hg in skin fibroblasts of green sea turtles through micronuclei formation (Finlayson et al., 2019). While the precise effects of lobed nuclei on erythrocyte function and overall organism health remain unclear, they underline the potential threats posed by Hg exposure. Additionally, other factors such as diseases like non-regenerative anaemia, could also play a role in the development of nuclear abnormalities in hawksbill sea turtles (Morão et al., 2024; Stacy et al., 2011).

Furthermore, as thoroughly discussed in Morão et al. (2024) other environmental contaminants, such as persistent organic pollutants (POPs), can be also contributing for the observed effects and thus future investigations should prioritize identifying and understanding the accumulation of additional contaminants in these turtles. For example, in a separate study involving loggerhead sea turtles, a correlation between carcinogenic polycyclic aromatic hydrocarbons (PAHs) and comet assay results was reported, indicating that the observed DNA fragmentation levels could be linked to these contaminants (Casini et al., 2018).

#### 4.3. Egg morphometric characteristics and yolk fatty acids

In terms of egg morphometric characteristics, the present study found slightly smaller measurements for egg diameter and whole egg weight compared to previous findings for the same species in Egypt ( $36.1\text{ mm} \pm 2.87$ ;  $31.0\text{ g} \pm 5.02$ ) (Hanafy, 2012), Seychelles ( $36.31\text{ mm} \pm 35.3$ ;  $25.5\text{ g}$ ) (Hitchins et al., 2004), and Malaysia ( $34.1\text{ mm}$ ) (Chan et al., 1999). These small differences in egg diameter and weight among these hawksbill sea turtles from different areas are likely a result of a combination of maternal resources, nest environment and local variations (Miller, 1997; Sönmez, 2016; Wallace et al., 2006), all of which

interact to shape reproductive traits in these populations.

Although the specific mechanisms of lipid migration from the reproductive female to the eggs in reptiles are not yet fully understood, it is hypothesized that this process occurs during vitellogenesis. In vitellogenesis, yolk proteins such as vitellogenin and other lipoproteins are synthesized mostly in the liver (Hamann et al., 2002; Price, 2017), being then released into the mother's bloodstream, where they circulate throughout her body. During this process, lipids are packaged into these lipoproteins which are believed to facilitate the transport of lipids from the mother's body to the developing eggs (Kawazu et al., 2015). Once inside the eggs, the lipoproteins are processed, and the lipids are incorporated into the yolk, contributing to the yolk's composition, and providing essential components for embryonic development (Hamann et al., 2002; Hewavisenthi and Parmenter, 2002; Lawniczak and Teece, 2009; Price, 2017). However, further research is needed to unravel the intricate details of lipid migration in sea turtles and reptiles in general.

The yolk samples of the present hawksbill turtles predominantly contained SFA and MUFA fatty acids, followed by lower percentages of PUFA and HUFA, as was previously seen for the yolk of green sea turtles from the same region (Morão et al., 2024). The most significant differences between the two species from the same nesting region, were observed in the PF regarding MUFA ( $p < 0.001$ , Table S3.2), with the hawksbill turtle presenting 5 % more than the green turtle (25.33 % versus 30.54 %). These disparities between species could be attributed to their different diet, as green sea turtles have primarily an herbivorous diet during their adult stages, while hawksbill turtles have a carnivorous diet (Jones and Seminoff, 2013) richer in MUFA fatty acids (Zong et al., 2018). Furthermore, for PUFA in the NF ( $p = 0.02$ , Table S3.2), the hawksbill sea turtle exhibited nearly half the percentage observed for the green turtle (1.25 % for hawksbill turtle compared to 2.22 % of green turtle).

Slightly different values were observed for the ratio of SFA to unsaturated (UNSAT) fatty acids between the fractions ( $p = 0.004$ , Table 3). This ratio was similar to the previous study with green sea turtles, where the NF exhibited a SFA/UNSAT ratio of  $0.92 \pm 0.08$ , while the PF had a ratio of  $1.24 \pm 0.24$  (Morão et al., 2024). The SFA/UNSAT fatty acids ratio plays a vital role in oviparous species, influencing various aspects of their biology and development (Tocher, 2003).

This ratio significant implicates energy storage, membrane fluidity, and nutritional intake during embryo development. SFA fatty acids, being more energy-dense, serve as a concentrated source of stored energy for embryonic development (Tocher, 2003). On the other hand, the balance between SFA and UNSAT fatty acids affects the fluidity and flexibility of cell membranes, with UNSAT fatty acids contributing to maintaining optimal membrane structure and function during embryogenesis (De Carvalho and Caramujo, 2018; McKeegan and Sturme, 2012).

The yolk fatty acid composition, specifically the SFA/UNSAT ratio, plays a critical role in nutrient availability for the embryo in oviparous species, influencing the accessibility of essential nutrients necessary for proper growth and development (Izquierdo et al., 2001). In the present study, the polar fraction presented a higher SFA/UNSAT ratio, where SFA fatty acids can have a significant impact on cellular processes such as apoptosis and cellular proliferation (Lordan et al., 2017). Meanwhile, UNSAT fatty acids act as important precursors for the synthesis of eicosanoids, which are essential for maintaining the balance of FA composition within this fraction (Lordan et al., 2017).

Another key ratio within UNSAT fatty acids is the DHA/EPA. Docosahexaenoic acid (DHA) and eicosapentaenoic acid (EPA) are important long-chain HUFA fatty acids. The hawksbill sea turtles exhibited similar DHA/EPA ratios in both fractions ( $p = 0.12$ , Table 3), which were comparable to the previous study with green sea turtles. In that study, the NF exhibited a DHA/EPA ratio of  $1.21 \pm 0.52$ , while the PF had a ratio of  $1.19 \pm 0.71$  (Morão et al., 2024).

DHA plays a crucial structural role in biomembranes, particularly in neural tissues like the brain and eyes where it is a key component of

polar lipids (Luo et al., 2019). This makes DHA essential during rapid growth phases, as it supports tissue formation during embryogenesis (Luo et al., 2019). Meanwhile, EPA serves as a precursor to bioactive compounds such as eicosanoids like prostaglandins and leukotrienes, which are important for reproductive development (Blanvillain et al., 2010). EPA can also partially fulfill DHA requirements by converting into DHA (Jin et al., 2017). Thus, the DHA/EPA ratio plays a significant role in various physiological and biochemical pathways, potentially affecting growth and proper development.

#### 4.4. Influence of maternal blood contaminants on egg morphometry and yolk fatty acids

Eggshells of oviparous animals, such as sea turtles, contain and provide 60 % of calcium content essential for embryo development. In addition to serving as calcium reservoir, they also act as a protective barrier against microbial infection, regulate water and gas exchange, and as a mineral reserve contributing to the embryo's overall safety (Mendonça et al., 2023; Sahoo et al., 2009). Similarly, the membrane plays an important role in embryonic development, by facilitating respiration, as well as the transport of nutrients and calcium (Ahmed et al., 2022; Castilla et al., 2010). It also serves as a protective barrier, preventing dehydration and filtering out microorganisms (Jabalera et al., 2022).

The findings of the present study indicate that an increased concentration of selenium (Se) in this species is likely linked to an increase in general egg weight. This is linked to a thicker and heavier eggshell texture, while aluminum (Al) levels are associated with a heavier membrane. Selenium is present in various parts of turtle egg, including the eggshell, membrane, albumin and yolk (Perrault et al., 2013; Savoca et al., 2022). This element is essential for protecting developing turtle embryos from oxidative stress, supporting immune function, maintaining DNA integrity, and promoting overall embryonic development (Dahlen et al., 2022; Liu et al., 2020; Pappas et al., 2019; Pavlović et al., 2010). Previous research has demonstrated that Se plays a critical role in the health and viability of sea turtle eggs, influencing hatching success and hatchling survival (Perrault et al., 2011). In this context, although Se levels were not directly measured in the eggs in the present study, our findings suggest that elevated Se levels in the female's blood may be associated with increased eggshell thickness, potentially offering enhanced initial protection to the developing embryo against environmental stressors.

This idea aligns with findings from other species. For example, in alligators, shell thickness is known to affect the hatching rate, with eggs having thinner shells more likely to fail to hatch compared to eggs with thicker shells (Zhang et al., 2023). Similarly, studies have shown that metal exposure can interfere with eggshell biomineralization, leading to thinner shells. For instance, cadmium (Cd) intake in hens has been linked to thinner eggshells at higher exposure levels (Zhu et al., 2020). In species like the clapper rail, exposure to metals like Mg, Cu, Zn, Pb and Hg has been shown to reduce eggshell thickness and cause structural, negatively impacting reproductive success (Rodríguez-Navarro et al., 2002). Other pollutants, such as dichlorodiphenyltrichloroethane (DDT), which has been shown to affect eggshell thickness in birds (Lesch et al., 2024), might exert similar effects in turtles due to the comparable chemical properties between species (Gautron et al., 2021; Morão et al., 2024).

On the other hand, higher levels of Al, a non-essential element, were associated with increased membrane weight. While this increase can offer structural support and enhance nutrient and moisture retention (Castilla et al., 2010), aluminum's toxicity suggests it might also disrupt gas exchange and further complicate development. For example, exposure in fish ultimately results in a block of ion exchange and respiration (Barabasz et al., 2002) and exposure to aluminium chloride in fertilised chicken egg led to decreased crown-rump length, elevated embryonic mortalities, delayed growth, and congenital heart defects (ElMazoudy

and Bekhet, 2016). Lead is a heavy metal known for its toxicity in reproduction (Kumar, 2018) and here it appears that an increase in Pb levels seems to be linked to a decrease in egg diameter (Table S2.4.1). This effect has been observed in pigeons, where Pb decreased both egg weight and length, resulting in smaller hatchlings with reduced survival rates (Williams et al., 2017). This aligns with findings in sea turtles, where larger eggs produce larger and more fit hatchlings with higher survival chances (Le Gouvello et al., 2020). Additionally, Pb has a higher affinity than calcium for protein binding sites due to its larger ionic radius, electronegativity, and irregular charge distribution, which disrupts calcium metabolism (Nwobi et al., 2021) and this interference can adversely affect eggshell quality (Sály et al., 2004). The reduced egg diameter may suggest that Pb competes with calcium during egg formation, leading to fewer carbonates in the eggs and thus smaller eggs. Smaller eggs, possibly with fewer reserves (fatty acids in the yolk), may have less reproductive success and/or produce more vulnerable hatchlings, but further research is needed for a better understanding of these processes and the possible consequences of the presence of Pb in females' blood on hatchlings.

Regarding fatty acid (FA) reserves, the neutral fraction of yolk's lipids, which consists of significant energy reserves in the form of triacylglycerols, plays a critical role in supplying the necessary energy for embryonic development. On the other hand, the yolk's polar fraction contains a large content of essential fatty acids contained in phospholipids that readily contribute to tissue formation and the development of cell membranes. All these lipids are vital for the structural integrity and functionality of cells during embryogenesis (Lawniczak and Teece, 2009; Morão et al., 2024). The present results showed that more pronounced and specific effects of the metals were seen in the PF of the sea turtle's egg yolk. As a result, the discussion will emphasize the FA profiling obtained in this fraction and their relation to contaminant load (Table S2.5.2 in supplementary material and Fig. 3C and D).

Hawksbill sea turtles do not feed during the nesting period, and they metabolize the accumulated reserves throughout their multiple nesting activities. These reserves sustain them during vitellogenesis and migration to and from the nesting area, which can be hundreds of miles (Santos et al., 2010). Similarly, metals are mobilized and metabolized at the same time as these reserves during vitellogenesis and egg development. Key proteins such as vitellogenin, copper transporter protein, and lipovitellin play critical roles in transporting essential metals like Zn, Cu and Se to developing eggs (Falchuk and Montorzi, 2001; Riggio et al., 2002; Unrine et al., 2006). Metallothioneins help regulate metal homeostasis and detoxification, managing the transport of metals like Zn and Cu (Guirlet et al., 2008). However, toxic metals like Cd, Pb, and Hg can also be transported, potentially competing with essential metals and disrupting physiological processes (Ballatori, 2002; Zhu et al., 2020).

It is also important to mention that the fatty acid composition is influenced by the diet of the nesting females (Filimonova et al., 2016). Hawksbill sea turtles are mainly spongivorous (Meylan, 1988) but they also feed on zoanths, algae, and small crustaceans (Baumbach et al., 2022). Their dominant diet, the sponges, are a fundamental source of SFA (mainly 16:0 and 18:0) and MUFA (mainly 16:1 and 18:1) fatty acids (Mishra et al., 2015), which justifies their higher content of these FA as discussed before. However, besides the direct influence of the diet, results showed that the metal levels in the females during the nesting activities may have also influenced the metabolization of the reserves to their eggs, as seen by the negative correlations with SFA fatty acids. This could indicate that SFA fatty acids are being metabolized or converted into UNSAT fatty acids in response to the stress induced by metals. A general negative correlation was observed between the overall contamination index (PLI) and SFA fatty acids in the polar fraction, with particularly 16:0 and 18:0 fatty acids presenting lower levels with increasing general metal concentrations. In agreement with SFA fatty acids metabolization, a positive and significant correlation between the contaminant load (PLI), in particular with UNSAT fatty acids, was registered. This was consistent with the general positive influence trend

in the essential n-6 group, mostly influenced by Cu, Fe, and Hg concentrations, but also in n-7 and n-9 groups with Se concentrations. These correlations seem to indicate that certain fatty acids, such as HUFA (20:4 n6, arachidonic fatty acid, ARA) or the n-6 and MUFA (16:1 n7, palmitoleic acid), are possibly being synthesized from SFA fatty acids. This is supported by other studies that mention that these fatty acids are synthesized from SFA, such as stearic (18:0) and palmitic (16:0) acids, through the action of stearoyl-CoA desaturases (Lee et al., 2016).

A previous study with green sea turtles indicated that the yolk's n-3 fatty acid group in the phospholipid fraction was most negatively affected by metal levels in females' blood (Morão et al., 2024). Although similar reports specifically for sea turtles are lacking, other studies on marine animals have observed a decrease in SFA and an increase in highly HUFA due to metal exposure (Filimonova et al., 2016; Silva et al., 2017, 2021). In the present study on hawksbill sea turtles, this pattern is also noticeable. Due to metal exposure and detoxification processes, the liver can synthesize and release higher amounts of fatty acids from membranes, including HUFA like ARA, which are associated with inflammation (Innes and Calder, 2018) and stress (Qi et al., 2022) responses. At a certain extent, these fatty acids may become available and be integrated with lipids that are transported in lipoproteins to support embryo development in eggs (Na et al., 2018; Speake et al., 1998).

Unlike most heavy metals, Se is an essential trace element that also counteracts the toxicity of other heavy metals, as suggested by the present results. It plays an important structural and enzymatic function mainly as an integral part of the selenoenzymes, able to neutralize ROS and enhance antioxidant activity, protecting against lipid oxidation and/or antagonizes the toxicity of heavy metals through sequestration of these elements into biologically inert complexes (Li et al., 2023; Zwolak, 2020; Zwolak and Zaporowska, 2012). Also, selenium-dependent proteins (selenoproteins) were demonstrated to regulate eicosanoid biosynthetic pathways, in which ARA is involved as a precursor, which may also be the cause for a different influence of Se in this FA, comparatively to other metals (Mattmiller et al., 2013). Contrarily to most of the other metallic elements tested, Se also showed a positive correlation with MUFA, mostly C16 to C18 carbon chain length FAs. While the exact mechanism remains uncertain, evidence indicates that Se may play a role in regulating the activity of stearoyl-CoA desaturase (Chang et al., 2019; Ferreira et al., 2022) and thus possibly activating the production of 18-carbon FAs and thus controlling its levels within cells (Piccinin et al., 2019). This enzyme plays a crucial role in the biosynthesis of fatty acids by introducing double bonds into specific carbon positions within the fatty acid chain (Paton and Ntambi, 2009; Talley and Mohiuddin, 2023). Moreover, this enzyme facilitates the dispersions of these FAs within membrane phospholipids (Scaglia and Igal, 2005).

Although further studies are needed to assess the effects of metal contamination on reproductive outcomes, such as embryo development and hatchling success, as well as potential long-term generational impacts on the population, this study postulates that the evidenced influence of metals in FA composition and in egg morphometrics, already verified for the green sea turtles (Morão et al., 2024), may also have some implications on the egg quality and consequent further embryo development in nesting female hawksbills.

## 5. Conclusions

This study is the first attempt to assess metal levels and its possible effects on the critically endangered hawksbill sea turtles nesting in São Tom' Island. This study showed a possible link between Hg levels and higher genotoxicity in female erythrocytes, particularly through the presence of lobed nuclei. Furthermore, the findings concerning egg morphometric data suggest that higher Se concentrations in this species are linked to a thicker and heavier eggshell, crucial for protecting developing turtle embryos and enhancing hatchling survival. Elevated Al levels found, could be associated with a heavier membrane,

potentially offering structural support but posing risks to gas exchange and development due to toxicity. Lead levels linked to reduced egg diameter, likely disrupt calcium metabolism, resulting in smaller eggshell and quality, and potentially less viable hatchlings. The analysis of yolk fatty acids in the hawksbill sea turtles' eggs indicate that the two lipid fractions are composed predominantly by SFA and MUFA fatty acids, followed by HUFA and PUFA, where the phospholipid fraction demonstrated to be more indicative of the impacts caused by metals contamination than the larger TAG fraction.

Moreover, significant correlations were found between metal contamination levels in the blood and alterations in the fatty acid profile and essential fatty acids which may indicate possible impacts on embryonic development of this critically endangered species of São Tomé Island. That is a major cause of concern in terms of species conservation, as it puts the future generations at risk and threatens the long-term viability of the population.

However, it is important to acknowledge that the limited sample size of this study may affect the generalizability of the findings. This underscores the need for future research with larger sample sizes to validate these patterns and strengthen the ecological insights derived from the results.

Current conservation efforts, such as nesting activities monitoring, protection and exhumation of nests, and awareness campaigns, are essential but could be enhanced by incorporating targeted ecotoxicological research such as this one. Furthermore, strengthening protection around critical feeding and nesting habitats is crucial, in which local NGOs have already been working by proposing the creation of a Marine Protected Area (MPA) in the south of São Tomé Island (Ferreira-Airaud et al., 2024). Enforcing policies to control pollutant runoff or discharge in these key areas could further reduce contamination risks, improving conservation outcomes. It would be equally important to identify the specific locations where these turtles are being exposed to contaminants. This would allow for more precise management strategies within the São Tomé and Príncipe archipelago and potentially across other regions where these turtles nest and face similar contamination threats. Such insights would significantly inform and enhance conservation strategies.

Future studies should implement continuous monitoring of metal contamination in hawksbill sea turtles, particularly Hg and Se levels, to assess the long-term trends. In addition to expanding the scope of contaminants analysed, assessing maternal transference of each contaminant from females' blood to the eggs, analysing other cellular parameters indicative of the organisms' health status, as well as including other developmental stages - such as hatchlings and/or juveniles or even adult males - would offer a more comprehensive picture of reproductive success and population health in relation to contamination. This broader, holistic approach is crucial for comprehending the impacts at higher biological levels and their significance and for refining conservation strategies to better safeguard these populations.

#### CRedit authorship contribution statement

**Inês F.C. Morão:** Writing – original draft, Methodology, Investigation, Formal analysis, Conceptualization. **Tiago Simões:** Writing – review & editing, Methodology, Investigation, Conceptualization. **Roger B. Casado:** Methodology, Investigation. **Sara Vieira:** Writing – review & editing, Investigation. **Betânia Ferreira-Airaud:** Writing – review & editing, Investigation. **Iliaria Caliani:** Writing – review & editing, Methodology, Investigation. **Agata Di Noi:** Writing – review & editing, Methodology, Investigation. **Silvia Casini:** Writing – review & editing, Methodology. **Maria C. Fossi:** Writing – review & editing, Resources. **Marco F.L. Lemos:** Writing – review & editing, Supervision, Resources, Methodology, Funding acquisition, Conceptualization. **Sara C. Novais:** Writing – review & editing, Supervision, Resources, Project administration, Methodology, Investigation, Formal analysis, Conceptualization.

#### Declaration of competing interest

The authors declare that they have no known competing financial interests or personal relationships that could have appeared to influence the work reported in this paper.

#### Acknowledgements

This study was supported by the Fundação para a Ciência e a Tecnologia (FCT) through the Strategic Project granted to MARE (UID/04292/MARE-Centro de Ciências do Mar e do Ambiente), the project granted to the Associated Laboratory ARNET (<https://doi.org/10.54499/LA/P/0069/2020>), the grant awarded to Inês Morão (<https://doi.org/10.54499/PD/BD/150562/2019>), and contracts to Tiago Simões (<https://doi.org/10.54499/2021.02559.CEECIND/CP1671/CT0001>) and Sara Novais (<https://doi.org/10.54499/CEECINST/00060/2021/C.P2902/CT0007>). We are grateful to all the members of the NGOs Programa Tatô and Fundação Príncipe, as well as NGO research assistants (biologists Maria Branco and Yedda Oliveira), and Marco Santos and Manuel Armindo José, who worked on Rolas Islet during the sampling period and assisted us in the field under challenging conditions.

#### Appendix A. Supplementary data

Supplementary data to this article can be found online at <https://doi.org/10.1016/j.envres.2025.121594>.

#### Data availability

Data will be made available on request.

#### References

- Ackerman, R., 1997. The nest environment and the embryonic development of sea turtles. In: Lutz, P.L., Musick, J.A. (Eds.), *The Biology of Sea Turtles*, I. CRC Press, pp. 83–106. <https://www.researchgate.net/publication/265270095>.
- Afonso, F., Félix, P.M., Chainho, P., Heumüller, J.A., de Lima, R.F., Ribeiro, F., Brito, A.C., 2022. Community perceptions about mangrove ecosystem services and threats. *Reg. Stud. Mar. Sci.* 49. <https://doi.org/10.1016/j.rsma.2021.102114>.
- Afonso, F., Palma, C., Brito, A.C., Chainho, P., de Lima, R., Heumüller, J.A., Ribeiro, F., Félix, P.M., 2023. Metal and semimetal loadings in sediments and water from mangrove ecosystems: a preliminary assessment of anthropogenic enrichment in São Tomé Island (Central Africa). *Chemosphere* 334 (March). <https://doi.org/10.1016/j.chemosphere.2023.138973>.
- Ahmed, T.A.E., Cordeiro, C.M.M., Elebute, O., Hincke, M.T., 2022. Proteomic analysis of chicken chorioallantoic membrane (CAM) during embryonic development provides functional insight. *BioMed Res. Int.* <https://doi.org/10.1155/2022/7813921>, 2022.
- Akinleye, A., Oremade, O., Xu, X., 2024. Exposure to low levels of heavy metals and chronic kidney disease in the US population: a cross sectional study. *PLoS One* 19 (4 April), 1–11. <https://doi.org/10.1371/journal.pone.0288190>.
- Amorim, N.P.L., de Assis, R.A., dos Santos, C.G.A., Benvido-Souza, M., Borges, R.E., de Souza Santos, L.R., 2024. Erythrocyte recovery in *Oreochromis niloticus* fish exposed to urban effluents. *Bull. Environ. Contam. Toxicol.* 112 (1), 15. <https://doi.org/10.1007/s00128-023-03833-2>.
- Angulo, E., 1996. The tomlinson pollution load index applied to heavy metal, "mussel-watch" data: a useful index to assess coastal pollution. *Sci. Total Environ.* 187 (1), 19–56. [https://doi.org/10.1016/0048-9697\(96\)05128-5](https://doi.org/10.1016/0048-9697(96)05128-5).
- Arantes, L.S., Vargas, S.M., Santos, F.R., 2020. Global phylogeography of the critically endangered hawksbill turtle (*Eretmochelys imbricata*). *Genet. Mol. Biol.* 43 (2), 1–12. <https://doi.org/10.1590/1678-4685-GMB-2019-0264>.
- Ballatori, N., 2002. Transport of toxic metals by molecular mimicry. *Environ. Health Perspect.* 110 (5), 689–694. <https://doi.org/10.1289/ehp.021105689>.
- Barabasz, W., Albińska, D., Jaśkowska, M., Lipiec, J., 2002. *Ecotoxicology of aluminium*. *Pol. J. Environ. Stud.* 11 (3), 199–203.
- Baumbach, D.S., Zhang, R., Hayes, C.T., Wright, M.K., Dunbar, S.G., 2022. Strategic foraging: understanding hawksbill (*Eretmochelys imbricata*) prey item energy values and distribution within a marine protected area. *Mar. Ecol.* 43 (2), e12703. <https://doi.org/10.1111/MAEC.12703>.
- Blanvillain, G., Owens, D.W., Kuchling, G., 2010. Hormones and reproductive cycles in turtles. *Hormones Reprod. Vertebrates: Reptiles* 3, 277–303. <https://doi.org/10.1016/B978-0-12-374930-7.10010-X>.
- Bligh, E.G., Dyer, W.J., 1959. A rapid method of total lipid extraction and purification. *Can. J. Biochem. Physiol.* 37 (8), 911–917. <https://doi.org/10.1139/O59-099>.
- Bridges, C.C., Zalups, R.K., 2017. Mechanisms involved in the transport of mercuric ions in target tissues. *Arch. Toxicol.* 91 (1), 63–81. <https://doi.org/10.1007/s00204-016-1803-y>.

- Canedo, A., de Jesus, L.W.O., Bailão, E.F.L.C., Rocha, T.L., 2021. Micronucleus test and nuclear abnormality assay in zebrafish (*Danio rerio*): past, present, and future trends. *Environ. Pollut.* 290, 118019. <https://doi.org/10.1016/j.envpol.2021.118019>.
- Casini, S., Calliani, I., Giannetti, M., Marsili, L., Maltese, S., Coppola, D., Bianchi, N., Campani, T., Ancora, S., Caruso, C., Furi, G., Parga, M., D'Agostino, A., Fossi, M.C., 2018. First ecotoxicological assessment of *Caretta caretta* (Linnaeus, 1758) in the Mediterranean Sea using an integrated nondestructive protocol. *Sci. Total Environ.* 631–632, 1221–1233. <https://doi.org/10.1016/j.scitotenv.2018.03.111>.
- Castilla, A.M., Van Dongen, S., Herrel, A., Francesch, A., Martínez De Aragón, J., Malone, J., José Negro, J., 2010. Increase in membrane thickness during development compensates for eggshell thinning due to calcium uptake by the embryo in falcons. *Naturwissenschaften* 97 (2), 143–151. <https://doi.org/10.1007/s00114-009-0620-z>.
- Castro, D., Mieirol, C.L., Coelho, J.P., Guilherme, S., Marques, A., Santos, M.A., Duarte, A. C., Pereira, E., Pacheco, M., 2018. Addressing the impact of mercury estuarine contamination in the European eel (*Anguilla Anguilla* L., 1758) – an early diagnosis in glass eel stage based on erythrocytic nuclear morphology. *Mar. Pollut. Bull.* 127, 733–742. <https://doi.org/10.1016/j.marpolbul.2017.12.028>.
- Cerriaco, L.M.P., Santos, B.S., de Lima, R.F., Bell, R.C., Norder, S.J., Melo, M., 2022. Physical geography of the Gulf of Guinea Oceanic Islands. In: Cerriaco, L.M.P., de Lima, R.F., Melo, M., Rayna, B.C. (Eds.), *Biodiversity of the Gulf of Guinea Oceanic Islands*. Science and Conservation. Springer, pp. 535–554. [https://doi.org/10.1007/978-3-031-06153-0\\_2](https://doi.org/10.1007/978-3-031-06153-0_2).
- Chan, E.H., Joseph, J., Liew, H.C., 1999. A study on the hawksbill turtles (*Eretmochelys imbricata*) of Pulau Gulisaan, Turtle Islands Park, Sabah, Malaysia. *Sabah Parks Nature J.* 2, 11–22.
- Chang, C.H., Liao, H.X.Q., Hsu, F.L., Ho, C.T., Liao, V.H.C., 2019. N-Y-(l-Glutamyl)-l-Selenomethionine inhibits fat storage via the Stearoyl-CoA desaturases FAT-6 and FAT-7 and the selenoprotein TRXR-1 in *Caenorhabditis elegans*. *Mol. Nutr. Food Res.* 63 (4), 1800784. <https://doi.org/10.1002/mnfr.201800784>.
- Chen, C., Yu, H., Zhao, J., Li, B., Qu, L., Liu, S., Zhang, P., Chai, Z., 2006. The roles of serum selenium and selenoproteins on mercury toxicity in environmental and occupational exposure. *Environ. Health Perspect.* 114 (2), 297–301. <https://doi.org/10.1289/ehp.7861>.
- Cortés-Gómez, A.A., Morcillo, P., Guardiola, F.A., Espinosa, C., Esteban, M.A., Cuesta, A., Girondot, M., Romero, D., 2018. Molecular oxidative stress markers in olive ridley turtles (*Lepidochelys olivacea*) and their relation to metal concentrations in wild populations. *Environ. Pollut.* 233, 156–167. <https://doi.org/10.1016/j.envpol.2017.10.046>.
- da Silva, C.C., Klein, R.D., Barcarolli, I.F., Bianchini, A., 2016. Metal contamination as a possible etiology of fibropapillomatosis in juvenile female green sea turtles *Chelonia mydas* from the southern Atlantic Ocean. *Aquat. Toxicol.* 170, 42–51. <https://doi.org/10.1016/j.aquatox.2015.11.007>.
- Dahlen, C.R., Reynolds, L.P., Caton, J.S., 2022. Selenium supplementation and pregnancy outcomes. *Front. Nutr.* 9 (October), 1–7. <https://doi.org/10.3389/fnut.2022.1011850>.
- Day, R.D., Segars, A.L., Arendt, M.D., Duan, Y., Lee, A.M., Peden-Adams, M.M., 2007. Relationship of blood Mercury levels to health parameters in the loggerhead sea turtle (*Caretta caretta*). *Environ. Health Perspect.*, November. <https://doi.org/10.1289/ehp.9918>.
- De Carvalho, C.C.C.R., Caramujo, M.J., 2018. The various roles of fatty acids. *Molecules* 23 (Issue 10). <https://doi.org/10.3390/molecules23102583>.
- Ehsanpour, M., Afkhami, M., Khoshnood, R., Reich, K.J., 2014. Determination and maternal transfer of heavy metals (Cd, Cu, Zn, Pb and Hg) in the Hawksbill sea turtle (*Eretmochelys imbricata*) from a nesting colony of Qeshm Island, Iran. *Bull. Environ. Contam. Toxicol.* 92 (6), 667–673. <https://doi.org/10.1007/s01028-014-1244-3>.
- ElMazoudy, R.H., Bekhet, G.A., 2016. In ovo toxico-teratological effects of aluminum on embryonic chick heart and vascularization. *Environ. Sci. Pollut. Control Ser.* 23 (21), 21947–21956. <https://doi.org/10.1007/s11356-016-7461-z>.
- Ergene, S., Çavaş, T., Çelik, A., Köleli, N., Kaya, F., Karahan, A., 2007. Monitoring of nuclear abnormalities in peripheral erythrocytes of three fish species from the Goksu Delta (Turkey): genotoxic damage in relation to water pollution. *Ecotoxicology* 16 (4), 385–391. <https://doi.org/10.1007/s10646-007-0142-4>.
- Evans, R.H., 1996. An analysis of criterion variable reliability in conjoint analysis. *Percept. Mot. Skills* 82 (3), 988–990. <https://doi.org/10.2466/pms.1996.82.3.988>.
- Falchuk, K.H., Montorzi, M., 2001. Zinc physiology and biochemistry in oocytes and embryos. In: *Biometals*, 14. Springer, pp. 385–395. <https://doi.org/10.1023/A:1012994427351>. Issues 3–4.
- Ferreira, E.V., Júnior, J.G.C., Corrêa, G.S.S., Kiefer, C., Alencar, S.A.S., Viana, L.H., Cavalheiro, L.F., 2022. Effects of organic selenium-and chromium-enriched diets on performance, carcass characteristics, lipid profile and fat quality of finishing pigs in different weight ranges. *An Acad. Bras Ciênc* 94 (2), 1–14. <https://doi.org/10.1590/0001-376520220200509>.
- Ferreira, R.L., Ceia, F.R., Borges, T.C., Ramos, J.A., Bolten, A.B., 2018. Foraging niche segregation between juvenile and adult hawksbill turtles (*Eretmochelys imbricata*) at Príncipe island, West Africa. *J. Exp. Mar. Biol. Ecol.* 498, 1–7. <https://doi.org/10.1016/j.jembe.2017.10.005>.
- Ferreira-Airaud, B., Schmitt, V., Vieira, S., Rio, M.J., Neto, E., Pereira, J., 2022. The sea turtles of São Tomé and Príncipe: Diversity, distribution, and conservation status. In: Cerriaco, L.M.P., de Lima, R.F., Melo, M., Bell, R.C. (Eds.), *Biodiversity of the Gulf of Guinea Oceanic Islands: Science and conservation*. Springer International Publishing, pp. 535–553. [https://doi.org/10.1007/978-3-031-06153-0\\_20](https://doi.org/10.1007/978-3-031-06153-0_20).
- Ferreira-Airaud, B., Vieira, S., Branco, M., Pina, A., Soares, V., Tiwari, M., Witt, | Matthew, Castilho, R., Teodósio, A., Hawkes, L.A., Laboratories, H., 2024. Green and hawksbill sea turtles of Eastern Atlantic: new insights into a globally important rookery in the Gulf of Guinea. *Ecol. Evol.* 14 (3), e11133. <https://doi.org/10.1002/ece3.11133>.
- Filimonova, V., Gonçalves, F., Marques, J.C., De Troch, M., Gonçalves, A.M.M., 2016. Fatty acid profiling as bioindicator of chemical stress in marine organisms: a review. *Ecol. Indic.* 67, 657–672. <https://doi.org/10.1016/j.ecolind.2016.03.044>.
- Finlayson, K.A., Leusch, F.D.L., van de Merwe, J.P., 2016. The current state and future directions of marine turtle toxicology research. *Environ. Int.* 94, 113–123. <https://doi.org/10.1016/j.envint.2016.05.013>.
- Finlayson, K.A., Leusch, F.D.L., van de Merwe, J.P., 2019. Primary green turtle (*Chelonia mydas*) skin fibroblasts as an in vitro model for assessing genotoxicity and oxidative stress. *Aquat. Toxicol.* 207, 13–18. <https://doi.org/10.1016/j.aquatox.2018.11.022>.
- Fuentes, M.M.P.B., McMichael, E., Kot, C.Y., Silver-Gorges, I., Wallace, B.P., Godley, B.J., Brooks, A.M.L., Ceriani, S.A., Cortés-Gómez, A.A., Dawson, T.M., Dodge, K.L., Flint, M., Jensen, M.P., Komoroske, L.M., Kophamel, S., Lettrich, M.D., Long, C.A., Nelms, S.E., Patrício, A.R., et al., 2023. Key issues in assessing threats to sea turtles: knowledge gaps and future directions. *Endanger. Species Res.* 52, 303–341. <https://doi.org/10.3354/ESR01278>.
- Gatto, C.R., Robinson, N.J., Spotila, J.R., Paladino, F.V., Santidrián Tomillo, P., 2020. Body size constrains maternal investment in a small sea turtle species. *Mar. Biol.* 167 (12), 1–11. <https://doi.org/10.1007/s00227-020-03795-7>.
- Gautron, J., Stapan, L., Le Roy, N., Nys, Y., Rodriguez-Navarro, A.B., Hincke, M.T., 2021. Avian eggshell biomineralization: an update on its structure, mineralogy and protein tool kit. *BMC Mol. Cell Biol.* 22 (1), 1–17. <https://doi.org/10.1186/s12860-021-00350-0>.
- Goher, M.E., Hassan, A.M., Abdel-Moniem, I.A., Fahmy, A.H., El-Sayed, S.M., 2014. Evaluation of surface water quality and heavy metal indices of Ismailia Canal, Nile River, Egypt. *Egypt. J. Aquat. Res.* 40 (3), 225–233. <https://doi.org/10.1016/j.ejar.2014.09.001>.
- Guevara-Meléndez, A.M., Comas-García, M., Labrada-Martagón, V., 2023. Description and quantification of micronucleus and nuclear abnormalities in erythrocytes of the sentinel green turtle (*Chelonia mydas*) with fluorescence microscopy. *Mutat. Res. Genet. Toxicol. Environ. Mutagen* 887. <https://doi.org/10.1016/j.mrgentox.2023.503596>.
- Guirlet, E., Das, K., Girondot, M., 2008. Maternal transfer of trace elements in leatherback turtles (*Dermostochelys coriacea*) of French Guiana. *Aquat. Toxicol.* 88 (4), 267–276. <https://doi.org/10.1016/j.aquatox.2008.05.004>.
- Guo, X., 2016. Advances in gas chromatography. *InTechOpen*. <https://doi.org/10.5772/57016>.
- Hamann, M., Limpus, C.J., Whittier, J.M., 2002. Patterns of lipid storage and mobilisation in the female green sea turtle *Chelonia mydas*. *J. Comp. Physiol. B Biochem. Syst. Environ. Physiol.* 172 (6), 485–493. <https://doi.org/10.1007/s00360-002-0271-2>.
- Hanafy, M., 2012. Nesting of marine turtles on the Egyptian beaches of the Red Sea. *Egypt. J. Aquat. Biol. Fish.* 16 (2), 59–71. <https://doi.org/10.21608/ejafb.2012.2125>.
- Hawkes, L.A., Broderick, A.C., Godfrey, M.H., Godley, B.J., 2009. Climate change and marine turtles. *Endanger. Species Res.* 7 (2), 137–154. <https://doi.org/10.3354/esr00198>.
- Hewavisenithi, S., Parmenter, C.J., 2002. Egg components and utilization of yolk lipids during development of the flatback turtle *Natator depressus*. *J. Herpetol.* 36 (1), 43–50. [https://doi.org/10.1670/0022-1511\(2002\)036\[0043:ECAUOY\]2.0.CO;2](https://doi.org/10.1670/0022-1511(2002)036[0043:ECAUOY]2.0.CO;2).
- Hitchins, P.M., Bourquin, O., Hitchins, S., Piper, S.E., 2004. Biometric data on hawksbill turtles (*Eretmochelys imbricata*) nesting at Cousine Island, Seychelles. *J. Zool.* 264 (4), 371–381. <https://doi.org/10.1017/S0952836904005850>.
- Hites, R.A., 2019. Correcting for censored environmental measurements. *Environ. Sci. Technol.* 53 (19), 11059–11060. <https://doi.org/10.1021/acs.est.9b05042>.
- Horne, J.B., Frey, A., Gaos, A.R., Martin, S., Dutton, P.H., 2023. Non-random mating within an Island rookery of Hawaiian hawksbill turtles: demographic discontinuity at a small coastline scale. *R. Soc. Open Sci.* 10, 221547. <https://doi.org/10.1098/rsos.221547>.
- Hsu, L.L., Culhane, A.C., 2020. Impact of data preprocessing on integrative matrix factorization of single cell data. *Front. Oncol.* 10, 973. <https://doi.org/10.3389/fonc.2020.00973>.
- IBM Corp., 2023. IBM SPSS statistics 28.0.1.0. Retrieved January 22, 2024, from <http://www.ibm.com/support/pages/downloading-ibm-spss-statistics-28010>.
- Innes, J.K., Calder, P.C., 2018. Omega-6 fatty acids and inflammation. *Prostaglandins Leukot. Essent. Fatty Acids*. <https://doi.org/10.1016/j.plefa.2018.03.004>.
- Izquierdo, M.S., Fernández-Palacios, H., Tacon, A.G.J., 2001. Effect of broodstock nutrition on reproductive performance of fish. *Reprod. Biotechnol. Finfish Aquacult.* 197, 25–42. <https://doi.org/10.1016/b978-0-444-50913-0.50006-0>.
- Jabalera, Y., Dominguez-Gasca, N., Muñoz, A., Hincke, M., Jimenez-Lopez, C., Rodriguez-Navarro, A.B., 2022. Antimicrobial defenses of table eggs: importance of antibacterial proteins in egg white as a function of hen age in an extended production cycle. *Food Microbiol.* 107 (May). <https://doi.org/10.1016/j.fm.2022.104068>.
- Jannetto, P.J., Cowl, C.T., 2023. Elementary overview of heavy metals. *Clin. Chem.* <https://doi.org/10.1093/clinchem/hvad022>.
- Jin, M., Monroig, O., Lu, Y., Yuan, Y., Li, Y., Ding, L., Tocher, D.R., Zhou, Q., 2017. Dietary DHA/EPA ratio affected tissue fatty acid profiles, antioxidant capacity, hematological characteristics and expression of lipid-related genes but not growth in juvenile black seabream (*Acanthopagrus schlegelii*). *PLoS One* 12 (4), e0176216. <https://doi.org/10.1371/journal.pone.0176216>.
- Jones, T.T., Seminoff, J.A., 2013. Feeding biology advances from field-based observations, physiological studies, and molecular techniques. In: Wyneken, J., Lohmann, K.J., Musick, J.A. (Eds.), *The Biology of Sea Turtles Vol Iii, III*. CRC Press, pp. 211–248.



2022. Impact of heavy metals in eggs and tissues of *C. caretta* along the Sicilian Coast (Mediterranean Sea). *Environ. - MDPI* 9 (7). <https://doi.org/10.3390/environments9070088>.
- Scaglia, N., Igal, R.A., 2005. Stearoyl-CoA desaturase is involved in the control of proliferation, anchorage-independent growth, and survival in human transformed cells. *J. Biol. Chem.* 280 (27), 25339–25349. <https://doi.org/10.1074/jbc.M501159200>.
- Schaumburg, L.G., Poletta, G.L., Siroski, P.A., Mudry, M.D., 2012. Baseline values of micronuclei and comet assay in the lizard *Tupinambis merianae* (Teiidae, Squamata). *Ecotoxicol. Environ. Saf.* 84, 99–103. <https://doi.org/10.1016/j.ecoenv.2012.06.023>.
- Shalan, M.G., 2022. Amelioration of mercuric chloride-induced physiologic and histopathologic alterations in rats using vitamin E and zinc chloride supplement. *Heliyon* 8 (12), e12036. <https://doi.org/10.1016/j.heliyon.2022.e12036>.
- Shaw, K.R., Lynch, J.M., Balazs, G.H., Jones, T.T., Pawloski, J., Rice, M.R., French, A.D., Liu, J., Cobb, G.P., Klein, D.M., 2021. Trace element concentrations in blood and scute tissues from wild and captive Hawaiian Green Sea turtles (*Chelonia mydas*). *Environ. Toxicol. Chem.* 40 (1), 208–218. <https://doi.org/10.1002/ETC.4911>.
- Silva, C.O., Simões, T., Félix, R., Soares, A.M.V.M., Barata, C., Novais, S.C., Lemos, M.F.L., 2021. *Asparagopsis armata* exudate cocktail: the quest for the mechanisms of toxic action of an invasive seaweed on marine invertebrates. *Biology* 10 (3), 223. <https://doi.org/10.3390/biology10030223>.
- Silva, C., Simões, T., Novais, S.C., Pimparel, I., Granada, L., Soares, A.M.V.M., Barata, C., Lemos, M.F.L., 2017. Fatty acid profile of the sea snail *Gibbula umbilicalis* as a biomarker for coastal metal pollution. *Sci. Total Environ.* 586, 542–550. <https://doi.org/10.1016/j.scitotenv.2017.02.015>.
- Simões, T.N., Silva, A.C., Santos, A.M.M.S., Chagas, C.A., 2019. Heavy metals in *Eretmochelys imbricata*, Linnaeus, 1766 (Testudines: Cryptodira), coast of Brazil. *Ecotoxicol. Environ. Contam.* 14 (1), 65–72. <https://doi.org/10.5132/eec.2019.01.08>.
- Sönmez, B., 2016. An assessment of egg size in the green turtle (*Chelonia mydas*) on Samandağ Beach, Turkey. *Nat. Eng. Sci.* 1 (3), 33–41. <https://doi.org/10.28978/nesciences.286310>.
- Speake, B.K., Noble, R.C., Murray, A.M.B., 1998. The utilization of yolk lipids by the chick embryo. *Worlds Poult. Sci. J.* 54 (4), 331–334. <https://doi.org/10.1079/wps19980022>.
- Speer, R.M., Wise, C.F., Young, J.L., Aboueiisa, A.E.M., Martin Bras, M., Barandiaran, M., Bermúdez, E., Márquez-D'Acunti, L., Wise, J.P., 2018. The cytotoxicity and genotoxicity of particulate and soluble hexavalent chromium in leatherback sea turtle lung cells. *Aquat. Toxicol.* 198 (March), 149–157. <https://doi.org/10.1016/j.aquatox.2018.03.003>.
- Stacy, N.I., Alleman, A.R., Saylor, K.A., 2011. Diagnostic hematology of reptiles. *Clin. Lab. Med.* 31 (1), 87–108. <https://doi.org/10.1016/j.cll.2010.10.006>.
- Suzuki, K., Noda, J., Yanagisawa, M., Kawazu, I., Sera, K., Fukui, D., Asakawa, M., Yokota, H., 2012. Particle-induced X-ray emission analysis of elements in plasma from wild and captive sea turtles (*Eretmochelys imbricata*, *Chelonia mydas*, and *Caretta caretta*) in Okinawa, Japan. *Biol. Trace Elem. Res.* 148 (3), 302–308. <https://doi.org/10.1007/s12011-012-9375-z>.
- Talley, J.T., Mohiuddin, S.S., 2023. Biochemistry, fatty acid oxidation. In: StatPearls. StatPearls Publishing. <https://www.ncbi.nlm.nih.gov/books/NBK556002/>.
- Tanabe, L.K., Scott, K., Dasari, V., Berumen, M.L., 2022. An assessment of heavy metals in green sea turtle (*Chelonia mydas*) hatchlings from Saudi Arabia's largest rookery, Ras Baridi. *PeerJ* 10. <https://doi.org/10.7717/peerj.13928>.
- Tchounwou, P.B., Yedjou, C.G., Patlolla, A.K., Sutton, D.J., 2012. Heavy metals toxicity and the environment. In: *Molecular, Clinical and Environmental Toxicology*, pp. 133–164. [https://doi.org/10.1007/978-3-7643-8340-4\\_6](https://doi.org/10.1007/978-3-7643-8340-4_6).
- ter Braak, C.J.F., Smilauer, P., 2002. CANOCO reference manual and CanoDraw for windows user's guide: software for canonical community ordination. In: *Section on Permutation Methods*. Microcomputer Power, Ithaca, New York, p. 10 h <https://doi.org/citeulike-article-id:7231853>, Version 4.5.
- Thompson, M.B., Speake, B.K., 2002. Energy and nutrient utilisation by embryonic reptiles. *Comparative biochemistry and physiology - A molecular and integrative. Physiology* 133 (3), 529–538. [https://doi.org/10.1016/S1095-6433\(02\)00188-5](https://doi.org/10.1016/S1095-6433(02)00188-5).
- Tocher, D.R., 2003. Metabolism and functions of lipids and fatty acids in teleost fish. In: *Reviews in Fisheries Science*, 11. Taylor & Francis Group, pp. 107–184. <https://doi.org/10.1080/713610925>. Issue 2.
- Tomlinson, D.L., Wilson, J.G., Harris, C.R., Jeffrey, D.W., 1980. Problems in the assessment of heavy-metal levels in estuaries and the formation of a pollution index. *Helgol. Meeresunters.* 33 (1–4), 566–575. <https://doi.org/10.1007/BF02414780>.
- Unrine, J.M., Jackson, B.P., Hopkins, W.A., Romanek, C., 2006. Isolation and partial characterization of proteins involved in maternal transfer of selenium in the western fence lizard (*Sceloporus occidentalis*). *Environ. Toxicol. Chem.* 25 (7), 1864–1867. <https://doi.org/10.1897/05-598R.1>.
- van de Merwe, J.P., Hodge, M., Olszowy, H.A., Whittier, J.M., Ibrahim, K., Lee, S.Y., 2009. Chemical contamination of green turtle (*Chelonia mydas*) eggs in Peninsular Malaysia: implications for conservation and public health. *Environ. Health Perspect.* 117 (9), 1397–1401. <https://doi.org/10.1289/ehp.0900813>.
- Van Dyke, J.U., Griffith, O.W., 2018. Mechanisms of reproductive allocation as drivers of developmental plasticity in reptiles. In: *Journal of Experimental Zoology Part A: Ecological and Integrative Physiology*. John Wiley & Sons, Ltd. <https://doi.org/10.1002/jez.2165>.
- Villa, C.A., Flint, M., Bell, I., Hof, C., Limpus, C.J., Gaus, C., 2017. Trace element reference intervals in the blood of healthy green sea turtles to evaluate exposure of coastal populations. *Environ. Pollut.* 220, 1465–1476.
- Wallace, B.P., DiMatteo, A.D., Bolten, A.B., Chaloupka, M.Y., Hutchinson, B.J., Abreu-Grobois, F.A., Mortimer, J.A., Seminoff, J.A., Amoroch, D., Bjorndal, K.A., Bourjea, J., Bowen, B.W., Dueñas, R., Casale, P., Choudhury, B.C., Costa, A., Dutton, P.H., Fallabrino, A., Finkbeiner, E.M., et al., 2011. Global conservation priorities for Marine turtles. *PLoS One* 6 (9), e24510. <https://doi.org/10.1371/journal.pone.0024510>.
- Wallace, B.P., Sotherland, P.R., Tomillo, P.S., Bouchard, S.S., Reina, R.D., Spotila, J.R., Paladino, F.V., 2006. Egg components, egg size, and hatchling size in leatherback turtles. *Comp. Biochem. Physiol. Mol. Integr. Physiol.* 145 (4), 524–532. <https://doi.org/10.1016/j.cbpa.2006.08.040>.
- Williams, R.J., Tannenbaum, L.V., Williams, S.M., Holladay, S.D., Tuckfield, R.C., Sharma, A., Humphrey, D.J., Gogal, R.M., 2017. Ingestion of a single 2.3 mm lead pellet by laying roller pigeon hens reduces egg size and adversely affects F1 generation hatchlings. *Arch. Environ. Contam. Toxicol.* 73 (4), 513–521. <https://doi.org/10.1007/s00244-017-0406-9>.
- Yipel, M., Tekeli, İ.O., İşler, C.T., Altuğ, M.E., 2017. Heavy metal distribution in blood, liver and kidneys of Loggerhead (*Caretta caretta*) and green (*Chelonia mydas*) sea turtles from the Northeast Mediterranean Sea. *Mar. Pollut. Bull.* 125 (1–2), 487–491. <https://doi.org/10.1016/j.marpolbul.2017.08.011>.
- Zhang, N., Zhang, H., Fan, G., Sun, K., Jiang, Q., Lv, Z., Han, B., Nie, Z., Shao, Y., Zhou, Y., Zhang, B., Wu, X., Pan, T., 2023. Effects of eggshell thickness, calcium content, and number of pores in erosion craters on hatching rate of Chinese alligator eggs. *Animals* 13 (8). <https://doi.org/10.3390/ani13081405>.
- Zhu, M., Li, H., Miao, L., Li, L., Dong, X., Zou, X., 2020. Dietary cadmium chloride impairs shell biomineralization by disrupting the metabolism of the eggshell gland in laying hens. *J. Anim. Sci.* 98 (2), 1–41.
- Zhu, W., Zhang, J., He, K., Geng, Z., Chen, X., 2020. Proteomic analysis of fertilized egg yolk proteins during embryonic development. *Poult. Sci.* 99 (5), 2775–2784. <https://doi.org/10.1016/j.psj.2019.12.056>.
- Zong, G., Li, Y., Sampson, L., Dougherty, L.W., Willett, W.C., Wanders, A.J., Alsema, M., Zock, P.L., Hu, F.B., Sun, Q., 2018. Monounsaturated fats from plant and animal sources in relation to risk of coronary heart disease among US men and women. *Am. J. Clin. Nutr.* 107 (3), 445–453. <https://doi.org/10.1093/ajcn/nqx004>.
- Zwolak, I., 2020. The role of selenium in arsenic and cadmium toxicity: an updated review of scientific literature. In: *Biological Trace Element Research*, 193. Springer, pp. 44–63. <https://doi.org/10.1007/s12011-019-01691-w>. Issue 1.
- Zwolak, I., Zaporowska, H., 2012. Selenium interactions and toxicity: a review. In: *Cell Biology and Toxicology*, 28. Springer, pp. 31–46. <https://doi.org/10.1007/s10565-011-9203-9>. Issue 1.